COLORADO STATE
UNIVERSITY
FORT COLLINS COLORADO
80523

department of electrical engineering

APPLICATION OF ELECTROHYDRODYNAMIC PHENOMENA TO SPACE PROCESSING

Final Report

March, 1975

By

T. B. Jones

Department of Electrical Engineering

Colorado State University

Fort Collins, Colorado 80523

NASA Contract # NAS8-30250

Prepared for

George C. Marshall Space Flight Center
Marshall Space Flight Center
Alabama 35812

Application of Electrohydrodynamic Phenomena to Space Processing

Final Report

March, 1975

T. B. Jones
Department of Electrical Engineering
Colorado State University
Ft. Collins, CO 80523

NASA Contract #NAS8-30250

Prepared for

George C. Marshall Space Flight Center
Marshall Space Flight Center
Alabama 35812

TABLE OF CONTENTS

LIST OF FIGURES

Page

LIST OF TABLES

I. INTRODUCTION

A. Purpose of this Research Program

The objective of this research program has been to consider the potential application of electrohydrodynamic (EHD) effects in zero and reduced gravity space processing and manufacturing processes. Several applications of EHD in the zero-gravity environment of a spacecraft have already been studied, and these are reviewed in the next section (I.B). However, very little attention has been devoted to space processing applications.

The broad variety of known electrohydrodynamical effects, and the sometimes unique fluid handling capabilities which they manifest, suggest an extensive rather than intensive investigation. Thus, the approach taken has been to identify several interesting EHD space processing concepts and to study these theoretically and/or experimentally. The initially selected concepts are briefly described below.

(i) EHD unit separation processes - the use of nonuniform electric fields to achieve the separation of various components out of heterogeneous fluids.

(ii) EHD liquid handling and control - employment of the unique liquid handling capabilities of nonuniform electric fields to contain, transfer, and measure liquids in zero-gravity.

(iii) Electrostatic extrusion and fiber drawing - electric charge-field interactions utilized to draw fine fibers of materials normally susceptible only to "containerless" processing.

(iv) EHD crystal growth enhancement - electric field effects used to enhance (or possibly suppress) certain crystal growth phenomena.

(v) EHD mixing - use of bulk free charge or polarization forces to promote mixing of certain chemically active, immiscible, or otherwise inhomogeneous fluids.

The concepts (i), (ii), and (v) are quite basic, and could have applications in many different zero-gravity processes, whereas (iii) and (iv) are much more specific. The one-year period of this initial study has not provided the opportunity to investigate the more specific concepts as thoroughly as might have been possible given more time. This is particularly true of (iii), electrostatic extrusion. The crystal growth enhancement activity (iv) has also been limited, though an annotated bibliography of the literature of electric field-crystal growth effects has been prepared.

This report is intended to review significant findings concerning EHD space processing gleaned from experiments, literature readings, and theoretical considerations. Most of the conclusions drawn about EHD space processing are nonspecific, in that they do not refer to specific processes destined for space manufacturing implementation. Such generality is entirely consistent with the spirit of this investigation. The ultimate intention of this document therefore, is to introduce the capabilities of electrohydrodynamic unit separation, liquid handling/control, and mixing to industrial chemists, metallurgists, etc., who are working on specific zero-gravity processes. These workers may then recognize that EHD suggests a possible solution to a problem they have encountered. The report, written with this goal in mind, contains a review of previously proposed zero-gravity applications of EHD and also a brief discussion of the prominent electrohydrodynamical force effects.

B. Background

Zero-gravity applications of electrohydrodynamic phenomena have been considered in the recent past. Some of the more prominent concepts are reviewed here, because of their indirect relevance to EHD space processing.

1. Zero-Gravity Liquid Orientation

The polarization force exerted on dielectric liquids by a strong nonuniform electric field may be used to provide an artificial gravitational field to orient dielectric fluids in zero-gravity environments. Both static and dynamic liquid orientation is possible. Proposed spacecraft propellant tank applications have included slosh suppression [1,2], efficient propellant collection and tank drainage [3], and vapor pull-through suppression [4].

2. Boiling Heat Transfer

The enhancement of ebullient heat transfer processes by strong nonuniform electric fields has been known for many years. The application of the electric field at the heated surface defers the burn-out point to higher heat flux values and also increases the minimum film boiling point [5,6,7]. The effect overall is to increase the effective heat transfer coefficient throughout the boiling regime. In extra-terrestrial applications, where the absence of gravity would impede normal ebullient processes, electrohydrodynamics may be considered as a means of promoting boiling heat transfer.

3. Condensation Heat Transfer

EHD effects couple to condensing liquid films and may be utilized to promote pseudo-dropwise condensation [8]. In zero-gravity situations, electrohydrodynamic forces could be used to remove liquid from a condensing surface thereby enhancing condensation heat transfer.

4. Pumping and Mixing

Various pumping schemes are of possible relevance to zero-gravity applications, including ion drag [9] and surface traveling wave [10] mechanisms. Somewhat related to pumping is mixing. Hoburg is studying various bulk electric field coupling concepts and their relevance to earthbound and extra-terrestrial mixing problems [11].

5. Specific Device Applications

Several devices which have been developed or are presently under study utilize electrohydrodynamic phenomena. All of these have been developed with aerospace applications in mind. One device is the electrohydrodynamic heat pipe [12,13], which utilizes an electromechanical flow structure in place of a conventional capillary wick for axial liquid transport. Another is a cooling system concept for spacecraft environmental control [14]. A third device is a liquid oxygen converter [15].

C. Electrohydrodynamic Forces

The diversity of possible applications of electrohydrodynamic phenomena stems from the diverse manifestations of force effects exerted on dielectric fluids by electric fields. The classical force density expression, including free charge, polarization, and electrostrictive forces is

$$\overline{f}^{e} = \rho_f \overline{E} - \tfrac{1}{2} E^2 \nabla \varepsilon - \nabla \left[\frac{\rho}{2} \frac{\partial \varepsilon}{\partial \rho} E^2\right], \qquad (1.1)$$

where ρ_f = free charge density,

$\overline{E}$ = electric field,

ε = dielectric permittivity,

and ρ = dielectric fluid density.

In pumping and mixing applications, the free charge term ($\rho_f \bar{E}$) tends to dominate, while in the liquid orientation applications, the polarization term ($-\frac{1}{2} E^2 \nabla \varepsilon$) is significant. The third term describes electrostriction effects which are not of significance in any zero-gravity EHD applications considered here.

1. Free Charge Forces

Free charge forces arise when charge separation occurs in a fluid medium stressed by an electric field. The charge may be either induced or injected externally. A simple example is the ion-drag pump, illustrated in Fig. 1.1. Charges are injected into the fluid bulk by a localized breakdown process. These charges are driven by the imposed electric field toward the opposite electrode. The charges, typically attached to molecules or small impurity particles, transmit their force to the liquid bulk by viscous drag coupling, and the result is net fluid motion, or ion-drag pumping.

Another example of free charge forces at work occurs when an electric field is applied to an inhomogeneous medium. Inhomogeneities or discontinuities in the electric conductivity result in free charge buildup. This occurs at the vapor interface of a uniform dielectric, or in the bulk of a nonuniform dielectric. Once this distributed charge builds up, it can interact with the imposed electric field and/or its own induced electric field to produce fluid motions. These motions often tend to mix the fluid. Refer to Fig. 1.2.

2. Polarization Forces

The form of the polarization force term in Eq. (1.1) above suggests that it depends on inhomogeneities in the dielectric permittivity ε. It further suggests that the polarization force is singular at the

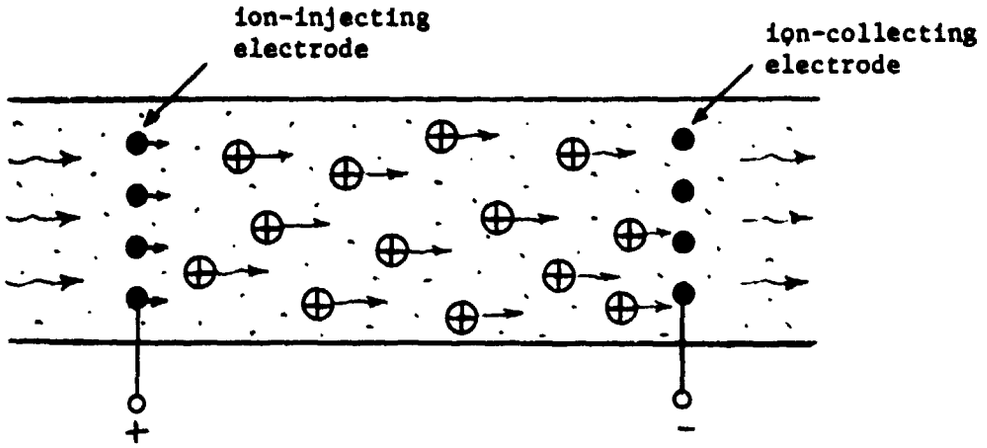

Figure 1.1 Ion-Drag Pumping Scheme. Up-stream electrode must have same sign as most easily created ion for a particular fluid.

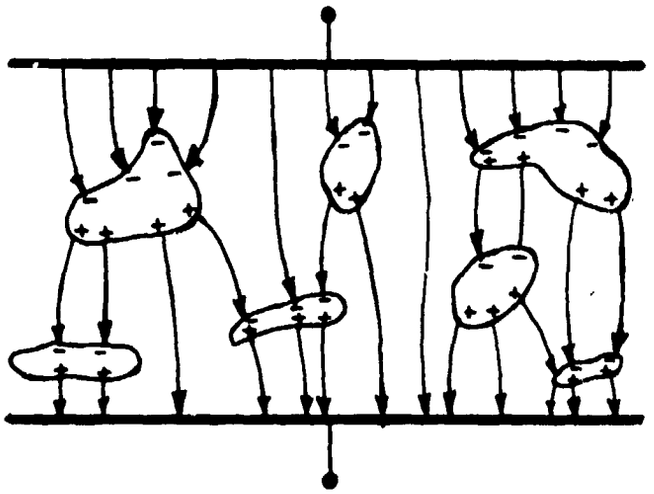

Figure 1.2 Electric Field Distortion due to inhomogenous liquid conductor. Bulk forces thus induced tend to promote mixing.

interface between incompressible fluids of differing permittivities, resulting in an effective discontinuity in hydrostatic pressure across an interface. This is only partially true; the most important condition requisite to observing polarization forces is a nonuniform electric field. In fact, the easiest and most complete phenomenological description of EHD polarization forces derives from the tendency of dielectric material of relatively higher polarizability to be drawn toward regions of higher electric field strength. Conversely, dielectric material of lower relative polarizability is expelled from regions of higher electric field strength. Several simple experimental demonstrations of this phenomenon serve as instructive examples.

In Fig. 1.3, two small dielectric spheres of dielectric permittivity ε_1 and ε_2 are located between diverging electrode plates which have been immersed in a third dielectric medium of permittivity ε_m. If we assume $\varepsilon_1 > \varepsilon_m$ and $\varepsilon_2 < \varepsilon_m$, then the polarization force

$$\overline{F}_1 = 2\pi r_1^3 \varepsilon_m \left(\frac{\varepsilon_1 - \varepsilon_m}{\varepsilon_1 + 2\varepsilon_m}\right) \nabla E^2 \qquad (1.2)$$

will tend to draw the sphere number 1 into the region of higher electric field, while the force

$$\overline{F}_2 = 2\pi r_2^3 \varepsilon_m \left(\frac{\varepsilon_2 - \varepsilon_m}{\varepsilon_2 + 2\varepsilon_m}\right) \nabla E^2 \qquad (1.3)$$

will tend to expel the sphere number 2. Typically, the sphere number 1 would be a solid sphere of dielectric material such that $\varepsilon_1 > \varepsilon_m$. The sphere number 2 would be a vapor or gas bubble with $\varepsilon_2 = \varepsilon_o < \varepsilon_m$. This effect is called "dielectrophoresis" by Pohl [16].

Another example of the polarization force is illustrated in Fig. 1.4, where various electrode configuration are shown with dielectric fluid

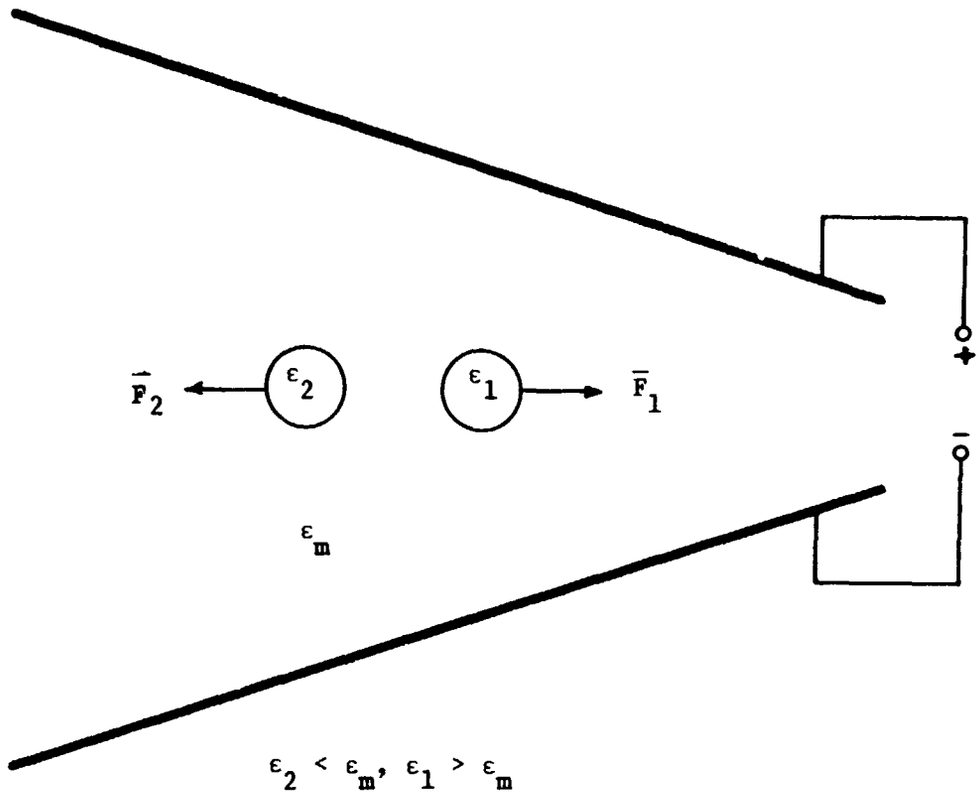

Figure 1.3 Illustration of Dielectrophoretic Force on Dielectric Particles in Non-uniform Electric Field. (Note $\bar{F}_1$, $\bar{F}_2$ are perpendicular to $\bar{E}$.)

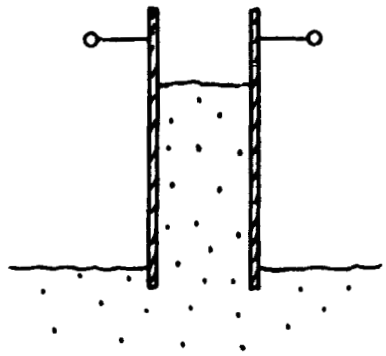

parallel-plate

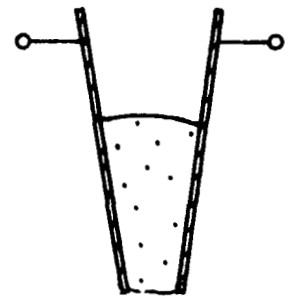

diverging-plate

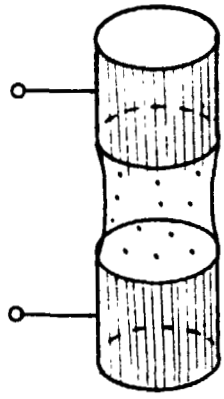

cylindrical

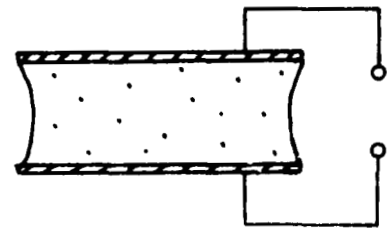

parallel-plate

Figure 1.4 Examples of Dielectric Liquid Orientation Using the Polarization Force Effect.

hydrostatically oriented in the high electric field regions. Note how the possible fluid configurations are limited only by the electrode structures and the electric field distribution they produce. These orientation schemes are characterized quantitatively by the body force ($-\frac{1}{2}E^2\nabla\varepsilon$) of Eq. (1.1). The resultant effective surface force, or effective pressure difference, may be equated to the hydrostatic head

$$\tfrac{1}{2}(\varepsilon - \varepsilon_o)\, E^2 = (\rho - \rho_o)gh \tag{1.4}$$

to determine the so-called dielectric height of rise h. The gravitational acceleration $g = 9.81\ m/sec^2$ may be replaced by acceleration a to predict the capability of an EHD dielectric fluid orientation scheme in a zero-gravity environment.

Still another example of the polarization force is the bulk force exerted on an inhomogeneous dielectric when subjected to a high frequency electric field. This force tends to induce turbulence and mixing.

The above discussion is not to be misconstrued as a review of all useful electrohydrodynamic force effects. There are many other phenomena which have not been considered. The only forces discussed have been those of direct relevance to the EHD space processing concepts studied. Other electrohydrodynamic phenomena not studied here might merit future consideration in space processing. These EHD effects include monolayer and double-layer interactions relevant to electrochemistry. An exhaustive discussion of electrohydrodynamics is found in a review article by J. R. Melcher [17].

II. ELECTROHYDRODYNAMIC UNIT SEPARATION PROCESSES

A capability of separating out various components of inhomogeneous fluids in zero-gravity environments is of possible significance in various space processing applications. McCreight and Griffin [18] have given initial feasibility consideration to three unit separation processes with potential application to chemical and biological purification. These are centrifuging, electrophoresis, and freeze-drying. It may be argued that electrophoresis is an electrohydrodynamic effect, and therefore within the scope of this study. However, the considerable efforts devoted by others to electropnoretic separation of biological components (in vaccines, etc.) precludes the need to study it here. Centrifuging is apparently not considered to have the potential in space processing manifested by freeze-drying or electrophoresis.

In this study, three distinct types of separation using dielectrophoresis (DEP) have been considered. These involve liquid-solid, liquid-liquid and liquid-gas systems. Liquid-solid separation was studied experimentally by Pohl as early as 1951 [16]. He successfully separated solid particles of carbon black filler from polyvinyl chloride in di-isopropyl ketone. It was his conclusion that separation of particles smaller than a few microns (10^{-6} meters) would not be practical due to the weak nature of the dielectrophoretic force in competition with thermal diffusion.

Separation of small liquid droplets out of a parent liquid was tried experimentally, with the result that the droplets distorted dramatically into long thin spikes. This distortion, due to the low liquid-liquid surface tension, masked out any effective DEP separation. It was concluded that liquid-liquid separation (of small droplets) is not a practical scheme.

Extensive experiments in the dielectrophoretic separation of gaseous and vapor bubbles were conducted, and the results show promise. The experiments are reviewed in section II. B.*

Dielectrophoresis may be of interest in several unit separation processes, including (i) the collection of undesirable gas/vapor bubbles trapped or evolved in liquid dielectrics including cryogens, and (ii) the removal of unwanted bubbles from certain molten plastic media. A related application of dielectrophoresis is (iii) the levitation and positioning of vapor bubbles in dielectric liquids, especially cryogenics.

A. Dielectrophoretic Separation

The dielectrophoretic force expression of Eq. (1.2) or (1.3) may be used to write an equation of motion for a spherical bubble of radius r and dielectric permittivity ε_b in an insulating fluid of permittivity ε_m.

$$\frac{4\pi r^3}{3}(\rho_b - \rho_m)\bar{g} + 2\pi r^3 \varepsilon_m \left(\frac{\varepsilon_b - \varepsilon_m}{\varepsilon_b + 2\varepsilon_m}\right) \nabla E^2 - C\eta r\bar{v} = 0, \qquad (2.1)$$

where $C = \begin{cases} 4\pi, & \text{fluid sphere model (pure liquid);} \\ 6\pi, & \text{solid sphere model (impure liquid).} \end{cases}$

This equation balances the gravitational (buoyant) force with the DEP force and viscous drag force (low Reynolds number limit). For bubbles, the coefficient C depends on whether the parent liquid is pure or impure. If the liquid is impure, a monolayer sometimes forms on the interface, and the bubble behaves like a solid sphere (Stokes drag)[20].

---

* More thorough documentation of these experiments and of appropriate theory is in preparation [19].

In the static case, $\bar{v} = 0$ and we can solve Eq. (2.1) for an effective gravitational acceleration g'.

$$g' = \left| \frac{3\varepsilon_m(\varepsilon_b - \varepsilon_m)\nabla E^2}{2(\rho - \rho_m)(\varepsilon_b + 2\varepsilon_m)} \right| \tag{2.2}$$

Equation (2.2) may be used for order of magnitude calculations of the force on a gas or vapor bubble.

Let

$$|\nabla E^2| \sim \frac{V^2}{s^3} \tag{2.3}$$

where V is the applied voltage and s is a characteristic dimension of the nonuniform electric field E. Then, if typical values for the fluid properties are employed ($\varepsilon_m \simeq 2.5\varepsilon_o$, $\varepsilon_b \simeq \varepsilon_o$, $\rho_m \simeq 10^3 kg/m^3$, $\rho_b \ll \rho_m$),

$$g' \sim 0.8\ V_{kv}^2 / s_{cm}^3, \tag{2.4}$$

where V_{kv} is expressed in kilovolts, s_{cm} is in centimeters, and g' is in centimeters/second^2. Equation (2.4) indicates that the DEP force on a bubble is significant with respect to gravity only for high voltages and/or small electrode dimensions and spacings. Furthermore, Eq. (2.4) does not reflect the limitations imposed by joulean heating and dielectric breakdown (see section III.A.3.). Because of the relatively weak nature of this force, it is important to emphasize the capabilities of the DEP force which make it unique.

B. Experiments

An experimental investigation has been conducted to verify experimentally theoretical models for the influence of nonuniform electric fields on gas bubbles in various dielectric fluids. While this research is not complete, the important results are reviewed here.

The experimental configuration shown in Fig. 2.1a allows a static measurement of the dielectrophoretic force by balancing it against the buoyancy of the bubble. A nitrogen gas bubble is released from below and rises up into the nonuniform horizontal electric field. The electric field gradient is positive upward, thus the DEP force on the bubble is downward. The bubble rises into the increasing electric field until the net force is zero, and the bubble stops. Actually, the bubbles do not remain midway between the plates, but tend toward one or the other electrode plate, where they remain until the voltage is turned off. The stationary position of the bubble is measured and compared to theory in Fig. 2.1b. The bubbles elongate slightly, as Garton and Krasucki observed [21], and the rather small effect of this elongation on the theoretical calculation is shown in the figure. Figure 2.1b illustrates the reasonably good correlation of the experimental data to the theoretical model for three different dielectric fluids in ac and dc electric fields.

Attempts to conduct similar experiments with tiny droplets of dielectric fluid were unsuccessful because the droplets elongated into needle shaped masses which tended to bridge the electrodes.

The diverging plate electrodes used to stop the bubbles are quite useful in the experimental verification of the theory, but they do not provide a practical means of controlling single bubbles in realistic situations. Another electrode structure, shown in Figure 2.2a, is much more promising. It consists of a ring electrode (below) and a disk electrode (above). When a bubble of nitrogen gas is released from below into a dielectric liquid, the bubble rises till it gets near the ring electrode where the electric field starts to act on it. If the electric field is strong enough, the bubble will come to rest on the electrode

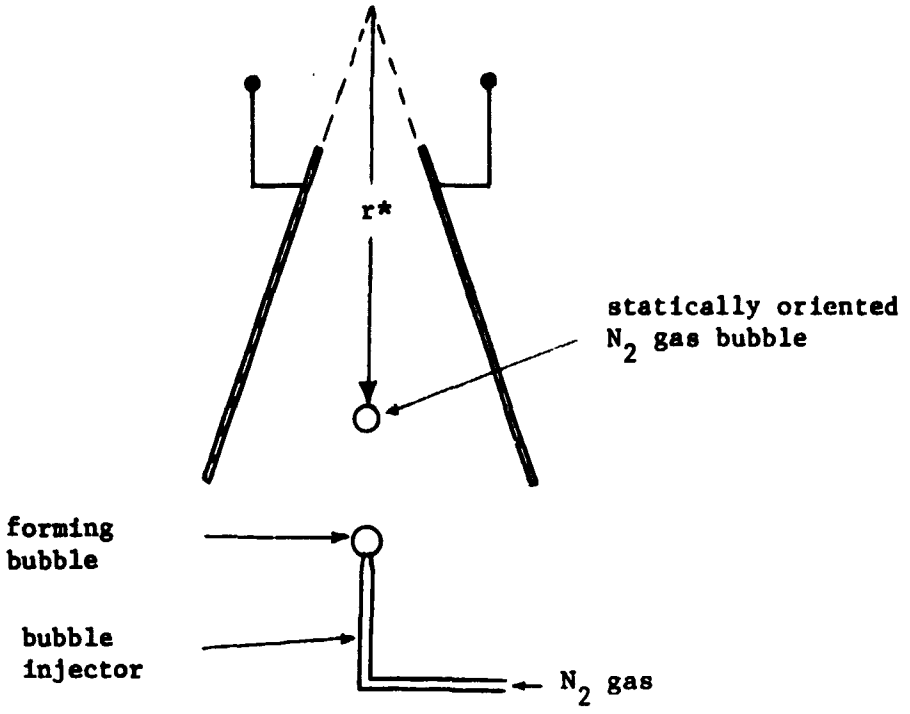

(a) Experimental Setup. Electrode structure is immersed in dielectric liquid.

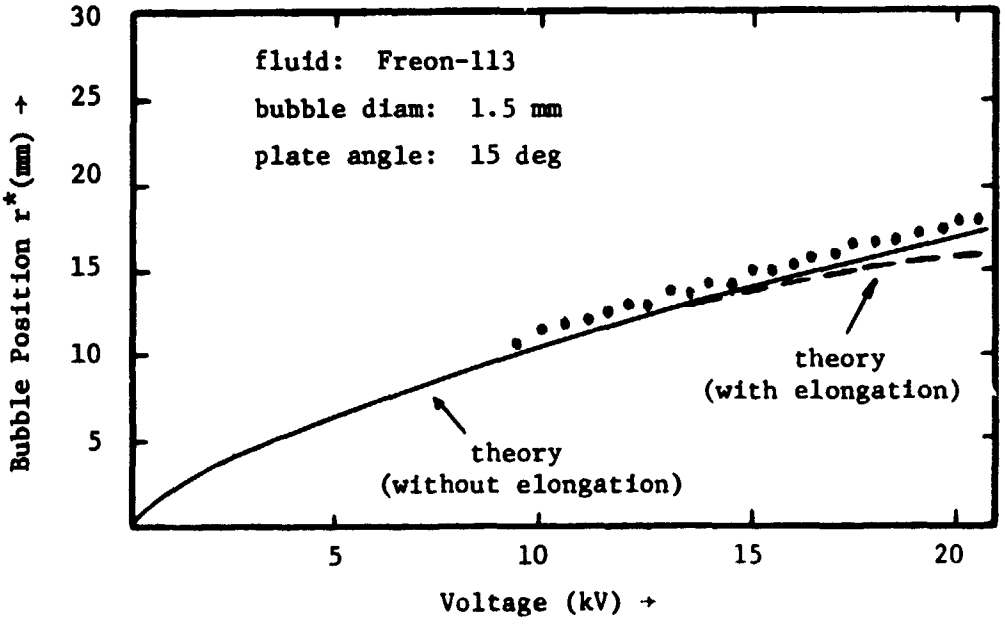

(b) Experimental Date and Theory

Figure 2.1 Static Dielectrophoretic Force Measurement Experiment

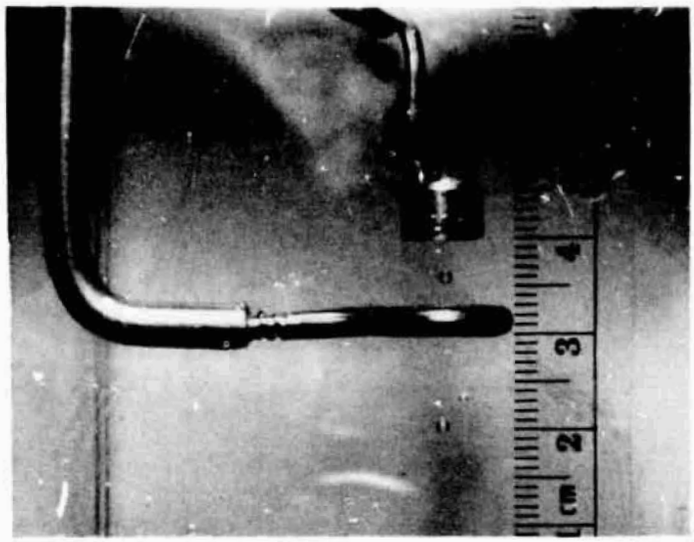

(fluid: Corn Oil)

(a) Bubble Levitator

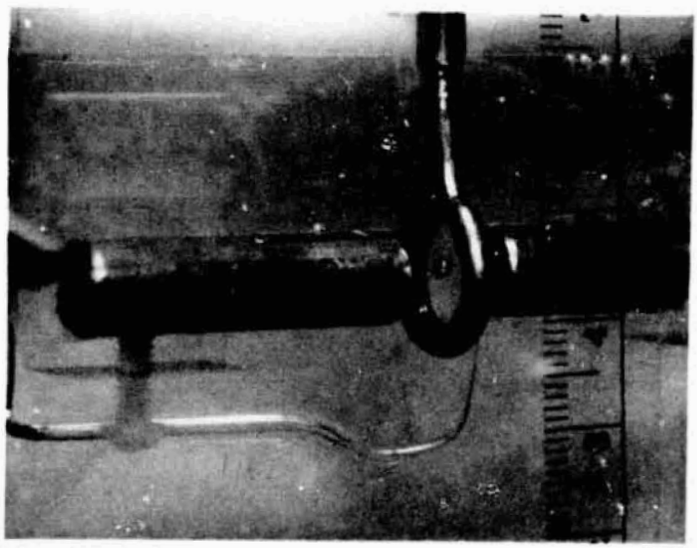

(fluid. Corn Oil)

(b) Bubble Positioner

Figure 2.2 Various Bubble Orientation Schemes (In both figures, gravity is downward).

system axis approximately midway between the ring and disk, as shown. The bubble stays centered due to the nature of the radial electric field gradient. By varying the voltage, the vertical equilibrium position of the bubble can be moved somewhat. A theoretical model for this practical bubble positioning geometry is presently being developed. The scheme shows promise in certain cryogenic and optical applications, where precision bubble positioning might be useful. Another electrode structure which can hold a bubble in zero-gravity is shown in Figure 2.2b.

Another experiment, shown in Fig. 2.3a provides a means of studying the bubble dynamics. The bubble is released between two divergent glass plates which have been treated with tin oxide to provide a transparent conductive coating. A voltage impressed between the conducting glass electrodes provides a nonuniform electric field which tends to push the bubbles outward (toward the weaker electric field). Thus, the bubbles prescribe a curved trajectory as shown in Fig. 2.3b. Independent experiments with rising nitrogen bubbles indicates that these bubbles in dielectric liquids such as transformer oil, corn oil, and Freon-113® behave essentially as solid spheres. Data plotted in Fig. 2.3b along with theoretical trajectories demonstrate reasonable correlation of experiments to the dynamic theory.

C. Conclusions

Without a specific space processing application proposed for dielectrophoretic unit separation, it is difficult to draw any but general conclusions based on our results. One general conclusion, which must be attributed primarily to the considerably earlier work of Pohl

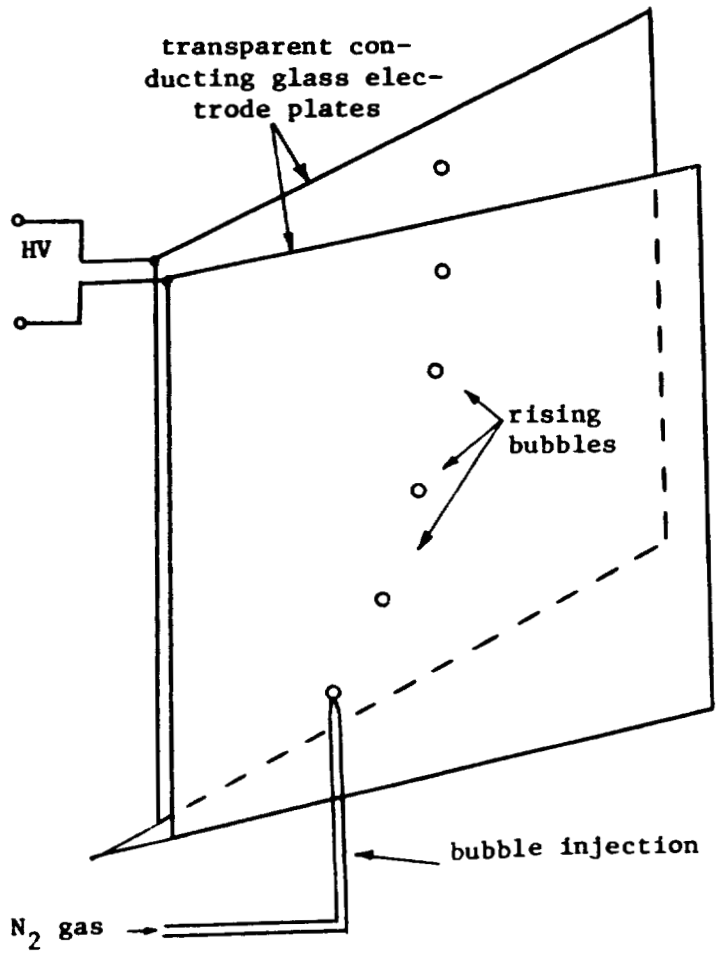

(a) Experimental Setup

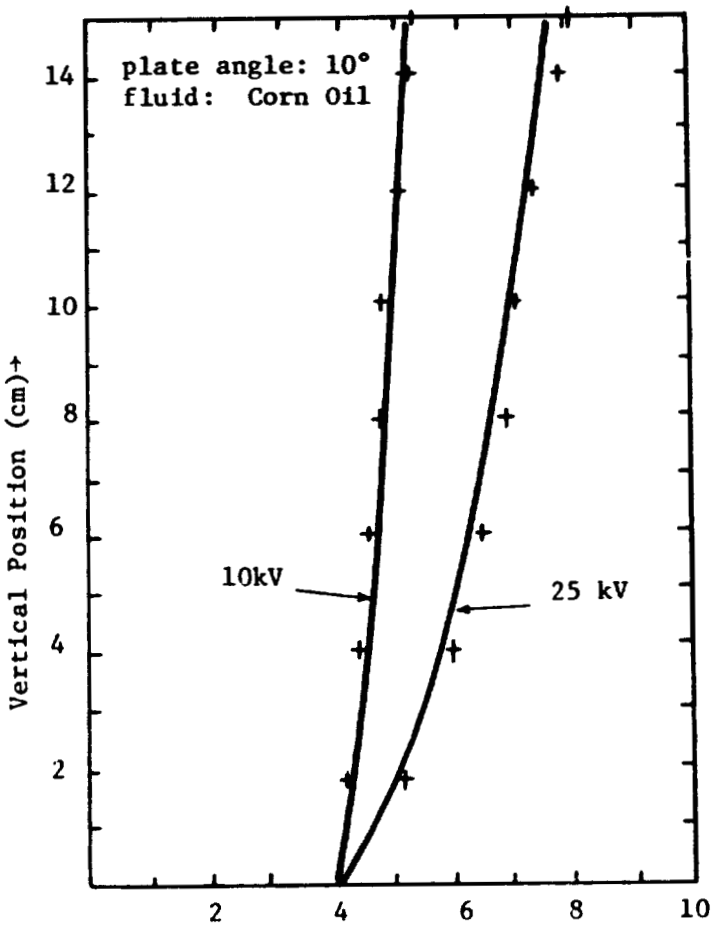

(b) Experimental Data and Theory (elongation included) for Dynamic Bubble Trajectory

Figure 2.3 Dynamic Dielectrophoresis Experiment

[16] is that there is a definite minimum size limit on particles which can be separated out by dielectrophoresis. For solid particles, this size limit is of the order of microns, and it is imposed by thermal motion. For bubbles, a similar thermally imposed minimum size limit of approximately one micron is imposed. Dielectrophoretic separation of bubbles smaller than the order of microns should therefore be ineffective.

Another conclusion is that DEP separation is restricted to insulating fluids and solids. This of course substantially limits the possible applications. Still, dielectrophoretic separation must be viewed as an alternative when electrophoresis is ineffective, which is sometimes the case in insulating fluids. It is also quite promising in cryogenic liquids.

1. Liquid-Solid Dielectrophoresis

In situations where insulating solid particles larger than ~ 1 micron are to be separated out of an insulating dielectric fluid, dielectrophoresis is an alternative to centrifuging or freeze-drying, at least when extremely high enrichments are not required.

2. Liquid-Liquid Dielectrophoresis

The experiments conducted with liquid-liquid dielectrophoresis indicate that moderately small dielectric liquid droplets are so distorted by the electric field that unit separation processes are probably not possible. For very small droplets (<< 1mm diameter), this elongation may not be as severe.

3. Liquid-Gas Dielectrophoresis

Primary attention in this study has been devoted to dielectrophoretic effects on gas bubbles in dielectric liquids. This force is

not very strong compared to normal terrestrial gravitation, but it presents a unique means of moving and controlling bubbles which neither centrifuging, electrophoresis, nor freeze-drying can achieve. Dielectrophoresis may be the only practical means of separating gas or vapor bubbles in insulating liquids.

Two possible problems with dielectrophoretic separation may hamper application of this effect. Some difficulty in controlling vapor bubbles produced by nucleate boiling was encountered. This was attributed to the inhomogeneities in the liquid dielectric produced by the heating. These inhomogeneities introduced the EHD mixing effects described above (section 1.B). The effect was more pronounced for dc electric fields than for ac. Another possible problem is the induced distortion of very large bubbles and the difficulty of moving such distorted bubbles by electrode structures of convenient size and configuration.

4. Bubble Purging in Molten Media

Dielectrophoresis offers a means of exerting a controllable force on unwanted bubbles found in molten media. This force might be used to purge such bubbles from such media, prior to solidification. The application of this technique to optical glass melts and to molded plastics in zero-gravity space processing is of some interest. No electrical conductivity or dielectric constant data for optical glasses or plastics in their molten states have been found, but data for typical glasses in their solid states is discouraging. Electrical conductivities appear to be too high to be consistent with practical high voltage power supply constraints. Bubble purging in optical glass melts does not show any promise, but in certain highly insulating plastics, dielectrophoresis may be applicable.

5. DEP in Cryogenic Liquids

Dielectrophoresis in cryogenic liquids deserves special mention because these liquids are ideal dielectrophoretic media (due to their excellent insulation and br akdown characteristics). Their dielectric constants are not high, however this is not a real problem in a zero-gravity environment. Cryogens are not true ohmic conductors; the very small currents measured in these liquids are strong functions of electrode configuration, indicating that uni-polar charge conduction dominates [22]. Thus, it is not meaningful to derive a joulean heating limit for these dielectrics.

Dielectrophoresis appears to offer some unique capabilities in the control of evolved vapor bubbles in a cryogenic liquid. In zero-gravity, evolving bubbles of vapor in a cryogenic liquid will not all naturally move toward a collection point unless some force is provided. Any space manufacturing scheme requiring a bubble-free cryogen may benefit from dielectrophoresis.

Laser fusion programs at Lawrence Livermore Laboratory (AEC) and elsewhere are proposing the use of hollow spheres of DT (deuterium tritide) as targets. The desired size of these target spheres ranges from 100 microns up to ~1. millimeter. Some difficulty in producing hollow spheres in this size range is to be anticipated. The utilization of dielectrophoresis to levitate and control DT vapor bubbles in a zero-gravity environment may offer a solution to this processing problem. The photographs in Fig. 2.2a,b show ~1 mm bubbles of nitrogen gas levitated in a dielectric fluid (in this experiment, Mazola corn oil). The same effect is obtainable in crogenic liquids. It is of interest to note that bubbles over a wide range of sizes (from ~.1 mm to ~2.0 mm) have been levitated in this way. Further, the variable voltage can be used to control the bubble position over a range of several millimeters.

III. ELECTROHYDRODYNAMIC LIQUID HANDLING AND CONTROL

The control of liquids in the zero-gravity environment of a spacecraft is not a trivial concern. In space processing applications, a need to contain, transfer, measure, and otherwise control liquids used in various processes may be anticipated. The polarization force discussed in section I.B.2 above offers a means of controlling a limited class of liquids, namely insulating dielectrics. This restriction to nonconductors is apparently severe because many liquids (e.g., water) are at least relatively good conductors. However, the severity of this limit on electrical conductivity depends on several factors including the allowable joulean heating, the choice of an ac electric field frequency, and the specific liquid orientation configuration. A more detailed discussion found in section III.A explains how the limit on the liquid electrical conductivity is established.

A. Static Liquid Orientation

1. Fluid Orientation Configurations

The great variety of possible liquid orientation configurations shown in Fig. 1.4 have the features in common that (1) the dielectric fluid collects in the high electric field region, (ii) the interface bulges into the fringing field, and (iii) the electric field is essentially tangential to the interface. In an ordinary laboratory environment, experimental study of liquid orientation with polarization forces is difficult due to severe atmospheric electrical breakdown limitations. A pressurized environment allows one to achieve very high electric field strengths ($\sim 10^7 \frac{\text{volts}}{\text{meter}}$) with common dielectrics ($\frac{\varepsilon}{\varepsilon_o} < 3$). The high pressure in effect simulates a reduced gravity environment by

reducing the ratio of gravitational to polarization body forces. The results of typical experiments in an environment of N_2 at ~ 250 psig are shown in Figure 3.1. Here are a collection of photographs of various electrode configurations with dielectric liquid oriented in the inter-electrode space.

The static dielectric liquid orientation problem can be separated into two prominent aspects, the hydrostatic equilibrium problem and the hydrodynamic stability problem. The details of equilibrium liquid profile calculations are not in the scope of this report; they are found elsewhere [23]. All of the configurations in Fig. 1.4 are stable to small disturbances. Such disturbances of the equilibrium are usually manifested as surface waves of small amplitude which resonate at a frequency inversely proportional to wavelength and which decay away due to viscous damping. These surface wave resonances may be important in zero-gravity liquid orientation applications if such a system is subject to vibrations at a frequency close to a resonance.

2. Fluid Orientation in Zero-Gravity

The performance of an electrohydrodynamic liquid container in zero-gravity is limited by its sensitivity to acceleration and/or vibration. The behavior of most dielectric liquid orientation geometries are quite similar and may be modelled by the very simple geometry shown in Fig. 3.2. Two parallel plates of dimensions ℓ and w are placed at a spacing s, and a voltage V is applied between them. A dielectric fluid of permittivity ϵ and density ρ is held between the plates by the polarization force. The liquid interface bulges into the fringing field E, which is assumed to have the spatial dependence shown in the figure.

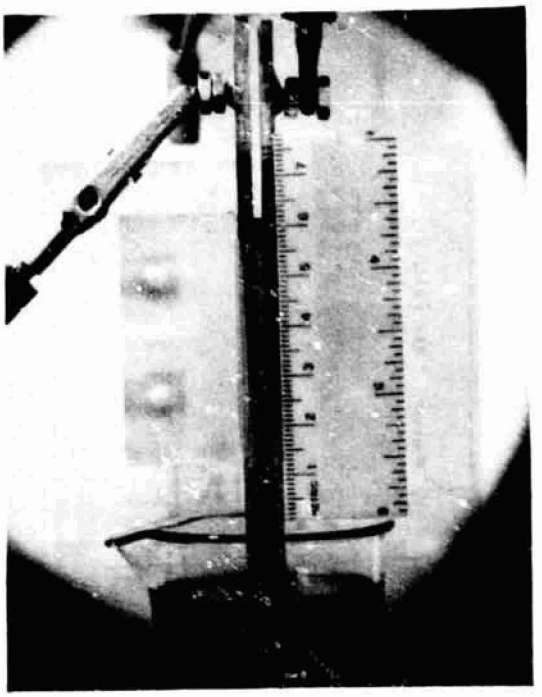

(a) Parallel-plate Geometry

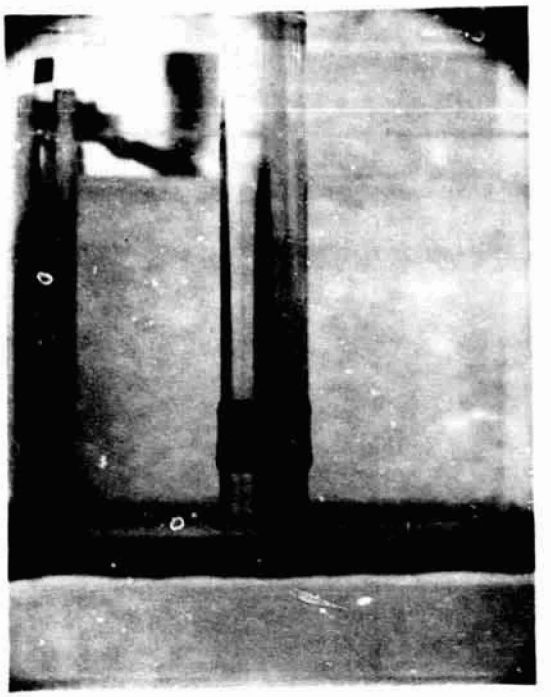

(b) Cylindrical Geometry

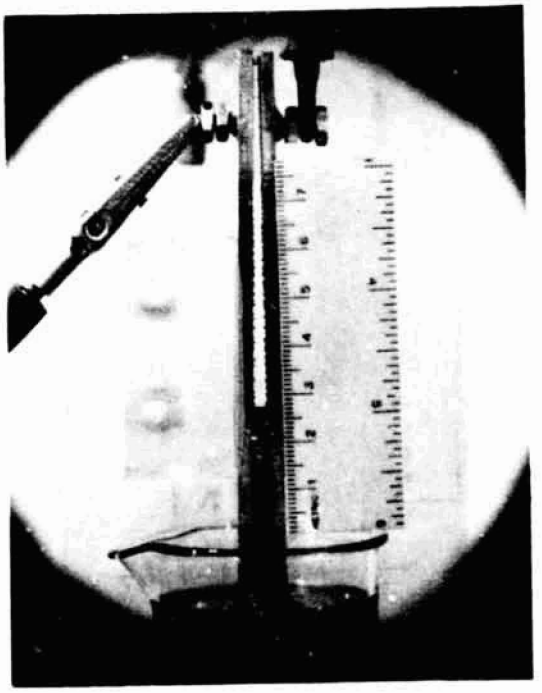

(c) Divergent-plate Geometry

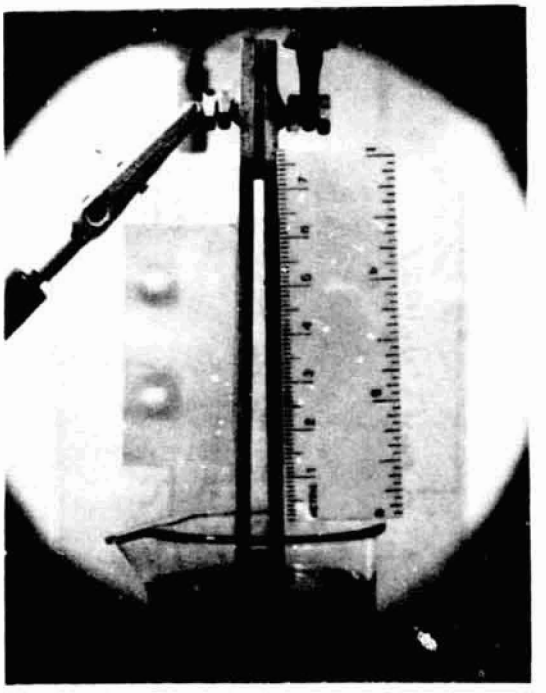

(d) Divergent-plate (fluid trapped at top)

Figure 3.1 Various Dielectric Fluid Orientation Geometries. Experiments performed in pressure vessel at ~250 psig dry N_2 gas.

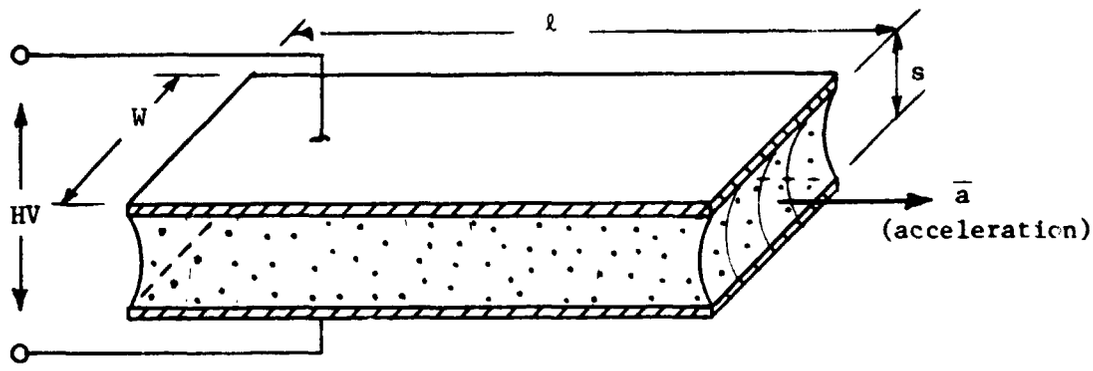

(a) Parallel-Plate System

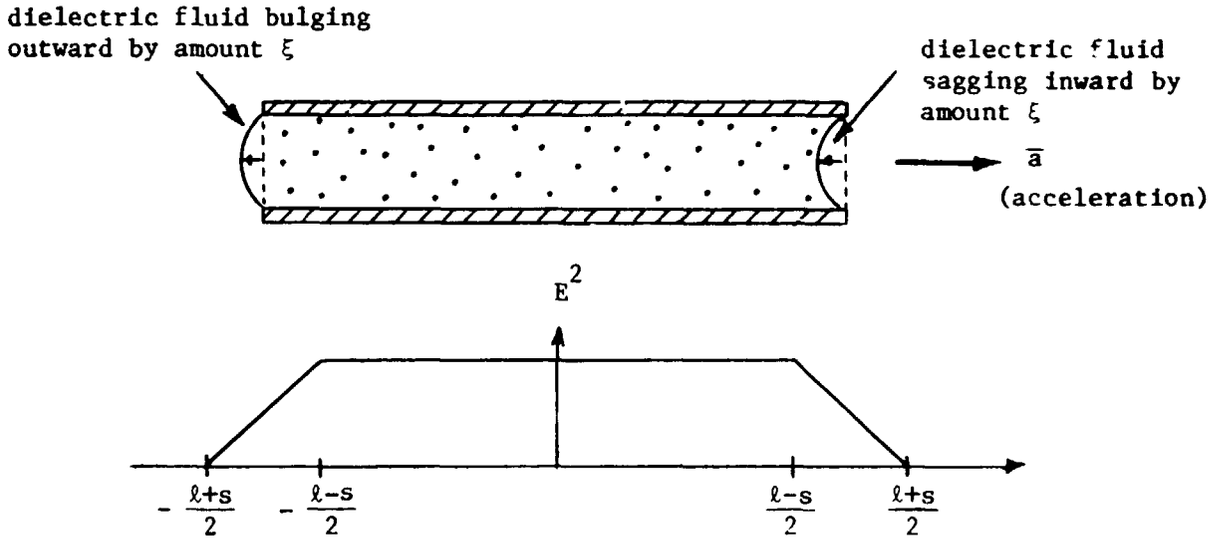

(b) Model of the Fringing Field Dependence

Figure 3.2 Parallel-Plate Dielectric Liquid System Geometry

We consider the effect of accelerating the system to the right at an acceleration $\bar{a}$ (m/sec^2) which is directed along the long axis of the electrodes. In response, the fluid mass will sag back an amount ξ which depends on the acceleration. Consider the frame of references at rest with respect to the electrodes. In this reference frame, there will be an apparent gravitational force tending to pull the fluid out from the electrodes to the left. Balancing the surface and pressure forces on the forward facing and backward facing interfaces:

$$p_{\ell 1} - p_o = - \frac{(\varepsilon - \varepsilon_o)}{2} E_o^2 \left[\frac{1}{2} + \frac{\xi}{s}\right], \tag{3.1}$$

$$p_{\ell 2} - p_o = - \frac{(\varepsilon - \varepsilon_o)}{2} E_o^2 \left[\frac{1}{2} - \frac{\xi}{s}\right], \tag{3.2}$$

where $E_o = V/s$ and $|\xi| \leq s/2$. However,

$$p_{\ell 1} + \rho a \ell = p_{\ell 2}, \tag{3.3}$$

and if we use Eq. (3.1), (3.2), and (3.3) we obtain:

$$\rho a \ell = (\varepsilon - \varepsilon_o) E_o^2 \frac{\xi}{s} \tag{3.4}$$

Equation (3.4) describes the static fluid response to a steady acceleration $\bar{a}$. Note that the inequality $|\xi| \leq s/2$ puts a limit on the maximum allowable acceleration a for a given system at a given voltage. If this inequality is violated, fluid is likely to be lost. When fluid loss occurs, the containment structure has failed.

Joulean heating and breakdown

Two important effects limit the maximum electric field which can be applied to a dielectric liquid to orient it. These are joulean heating and electrical breakdown. These limits may be illustrated

conveniently by using Eq. (3.4). The maximum acceleration the static EHD orientation structure of Fig. 3.2 can sustain at a given electric field E_o without probable fluid loss is determined by setting $\xi = s/2$ in Eq. (3.4). Thus,

$$(a\ell)_{max} = \frac{(\varepsilon - \varepsilon_o) E_o^2}{2\rho} \tag{3.5}$$

When an electric field $\bar{E}$ stresses a dielectric, the current density $\bar{J} = \sigma\bar{E}$ results in ohmic or joulean heating of the liquid bulk. The rate of power dissipation per unit volume is

$$P_{diss} = \bar{J} \cdot \bar{E} = \sigma E^2, \ (\frac{watts}{meter^3}) \tag{3.6}$$

where σ is the electrical conductivity. Using Eq. (3.5) and (3.6), we get

$$(a\ell)_{max} = \frac{(\varepsilon - \varepsilon_o)}{2\rho\sigma} P_{diss} \tag{3.7}$$

The quantity $(a\ell)_{max}$ is plotted versus P_{diss} in Fig. 3.3 for a number of dielectric fluids, ranging from highly insulating silicon oil (DC-200) to relatively conducting glycerine. The properties of the fluids used to perform the calculations are found in Table 3.1. Note that to sustain a given value of $(a\ell)_{max}$ for both Dow-Corning 200 series silicon oil and for glycerine, a rate of joulean heating approximately seven orders of magnitude higher must be sustained in the glycerine. This translates to an instantaneous heating rate which can be calculated as follows

$$\frac{dT}{dt} = \frac{P_{diss}}{\rho c}, \tag{3.8}$$

so that

$$(a\ell)_{max} = \frac{(\varepsilon - \varepsilon_o)c}{2\sigma} \cdot \frac{dT}{dt} \tag{3.9}$$

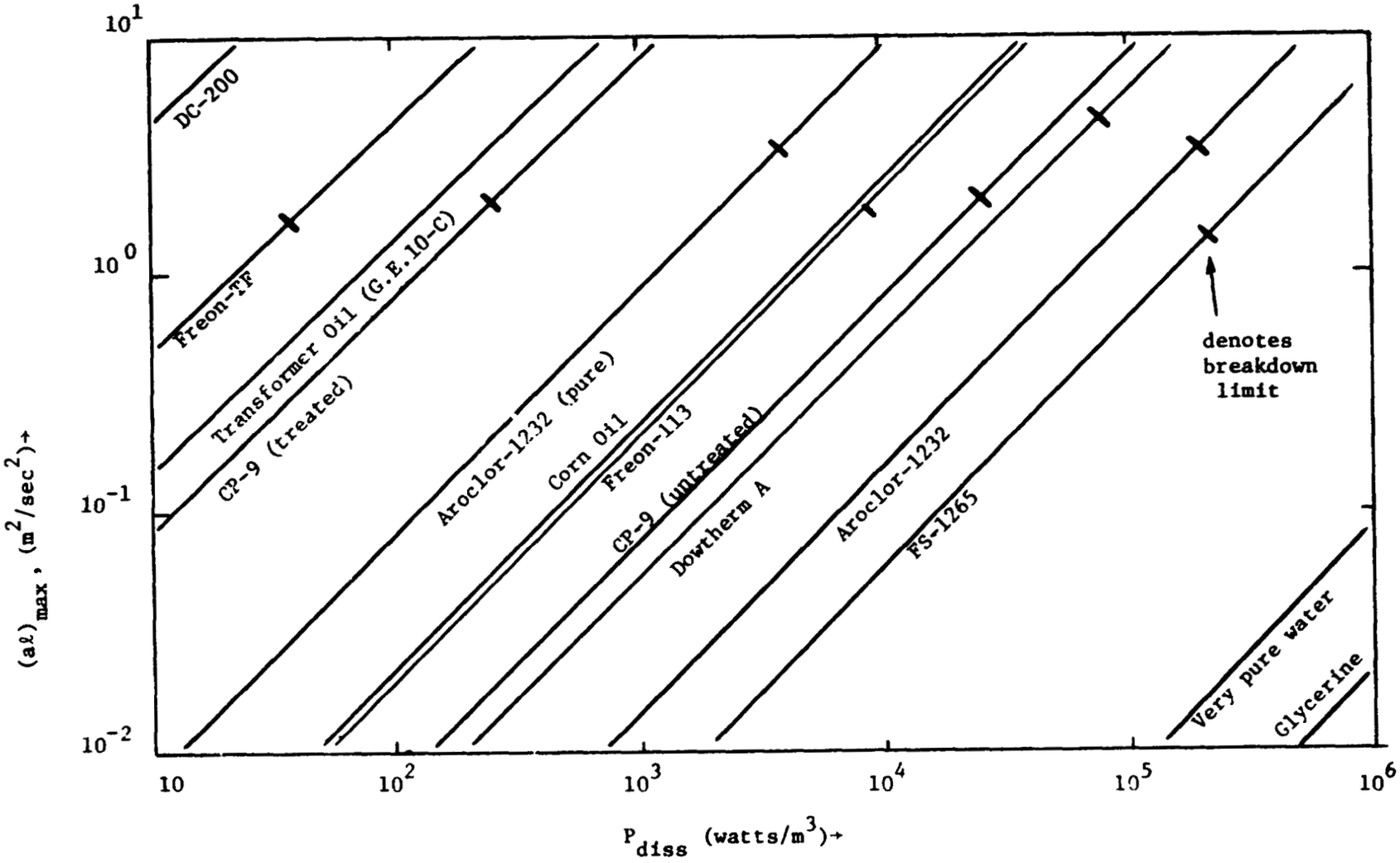

Fig. 3.3 Electrohydrodynamic Static Orientation Performance Measure of Various Dielectrics Versus Joulean Power Dissipation. Dielectric breakdown limit shown.

Table 3.1

Properties of Some Representative Dielectric Liquids Relevant to Electrohydrodynamic Space Processing (compiled from published and unpublished sources)

Fluid (manufacturer)	Dielectric Constant $\varepsilon/\varepsilon_o$	Conductivity (mhos/m) σ	Relaxation Time (sec) τ	Breakdown Strength (kV/cm) E_b	Liquid Density (kg/m^3) ρ	dynamic viscosity (kg/m-sec) μ	Surface tension (nt/m) γ
Freon-113 (Dupont)	2.41 (25°C)	$\sim 2 \cdot 10^{-11}$	~1.1	Liquid: 206.(25°C) Vapor: 156.(sat. 47°C)	$1.57 \cdot 10^3$ (25°C)	$.68 \cdot 10^{-3}$ (25°C)	.0173 (25°C)
Freon-12 (Dupont)	2.13 (29°C)	--	--	-- Vapor: 68.(latm. 73°F)	$1.31 \cdot 10^3$ (25°C)	$.396 \cdot 10^{-3}$ (-21.6°F) $.2 \cdot 10^{-3}$ (25°C)	.009 (25°C)
Dowtherm A (Dow)	3.26 (75°F)	$\sim 1.7 \cdot 10^{-10}$ (75°F)	.17 (75°F)	Liquid: 209.(75°F) --	$1.057 \cdot 10^3$ (75°F)	$3.8 \cdot 10^{-3}$ (25°C)	.040 (68°F)
DC-200 (10 centistoke) (Dow-Corning)	2.64 (23°C)	10^{-14} (?) (23°C)	>10(?) (23°C)	Liquid: 165(23°C) --	$.94 \cdot 10^3$ (23°C)	$9.4 \cdot 10^{-3}$ (23°C)	.020 (23°C)
FS-1265 (Dow-Corning)	6.95 (~25°C)	$3.3 \cdot 10^{-9}$ (~25°C)	.019 (~25°C)	Liquid: 79.(23°C) --	$1.25 \cdot 10^3$ (25°C)	.375 (25°C)	.0257 (23°C)
Corn Oil (Mazola)	3.1 (~25°C)	$\sim .5 \cdot 10^{-10}$ (~25°C)	~.55 (~25°C)	--	$0.91 \cdot 10^3$ (~25°C)	$5.46 \cdot 10^{-2}$ (~25°C)	.062 (~23°C)

Table 3.1 (Continued)

Fluid (manufacturer)	Dielectric Constant $\varepsilon/\varepsilon_o$	Conductivity (mhos/m) σ	Relaxation Time (sec) τ	Breakdown Strength (kV/cm) E_b	Liquid Density (kg/m^3) ρ	Dynamic viscosity (kg/m-sec) μ	Surface tension (nt/m) γ
Castor Oil	4.67 (~25°C)	--	--	--	$.96 \cdot 10^3$ (~25°C)	.99 (20°)	--
CP-9 (Monsanto)	2.66 (25°C)	Untreated 10^{-10} Treated: 10^{-12}	Untreated .24 Treated: 2.4	Liquid: 157 --	$.98 \cdot 10^3$ (25°C)	$4.35 \cdot 10^{-3}$ (100°F)	.038 (22°C)
Aroclor-1232 (Monsanto)	5.4-5.7 (25°C)	Manu.Data 2.10^{-11} (?) (25°C) Other Meas $1\text{-}3 \cdot 10^{-9}$ (25°C)	2.4(?) .016-.048	Liquid: 138.(25°C)	$1.27 \cdot 10^3$ (25°C)	~$5.5 \cdot 10^{-3}$ (100°F) <$1.3 \cdot 10^{-2}$ (210°F)	.047 (23°C)
Transformer Oil (GE 10C)	2.56 (25°C)	$<5 \cdot 10^{-13}$? (23°C	>40 (23°C)	--	$.87 \cdot 10^3$ (23°C)	~10^{-2} (23°C)	.04 (23°C)
Sulfur (Liquid)	3.52 (118°C)	--	--	--	$1.8 \cdot 10^3$	.0109 (123°C)	.039 (445°C)
Methyl Alcohol	32.6 (25°C)	~$7 \cdot 10^{-4}$ (25°C)	~$4 \cdot 10^{-7}$ (25°C)		$.785 \cdot 10^3$ (25°C)	$.547 \cdot 10^{-3}$ (25°C)	.0218 (30°C)
Glycerine	42.5 (25°C)	$6.4 \cdot 10^{-6}$ (25°C)	$5.9 \cdot 10^{-4}$ (25°C)		$1.26 \cdot 10^3$ (25°C)	.954 (25°C)	.063 (18°C)
H_2O	~78.5 (25°C)	Distilled $2 \cdot 10^{-4}$ UltraPure $4 \cdot 10^{-6}$	$3.5 \cdot 10^{-6}$ (18°C) $1.7 \cdot 10^{-4}$		10^3 (25°C)	10^{-3} (20°C)	.073 (18°C)

The Eq. (3.9) is plotted in Fig. 3.4. Note that the instantaneous heating rate in water and glycerine are completely unacceptable for reasonable values of $(a\ell)_{max} > 10^{-2} m^2/sec^2$. For this reason, water and most other polar dielectric media cannot be used in EHD liquid orientation applications.

Another limit is imposed on $(a\ell)_{max}$ by electrical breakdown. Liquids will sustain a maximum electrical stress E_b before breakdown occurs. This in effect limits the performance by putting an upper limit on the useable portion of the curves in Fig. 3.3 for each given liquid. These limits are calculated based on published liquid breakdown strengths contained in Table 3.1.

Charge relaxation

The charge relaxation time,

$$\tau = \frac{\varepsilon}{\sigma} \tag{3.10}$$

is the time constant associated with the buildup of electric charge at the interface of a finite conducting medium. For the liquid orientation schemes of Fig. 1.4, the only effect of charge relaxation is a surface instability mechanism for dc electric fields [24]. This instability results in a surface driven convection of liquid which is more pronounced in less viscous li ids. If liquid convection must be completely eliminated, then charge relaxation imposes the limit that the electric field alternate at a frequence f such that:

$$f >> \frac{1}{\tau} = \frac{\sigma}{\varepsilon} \tag{3.11}$$

Vibration at Resonances

If an EHD containment structure in a zero-gravity environment is subjected to strong vibrations at a frequency close to a surface

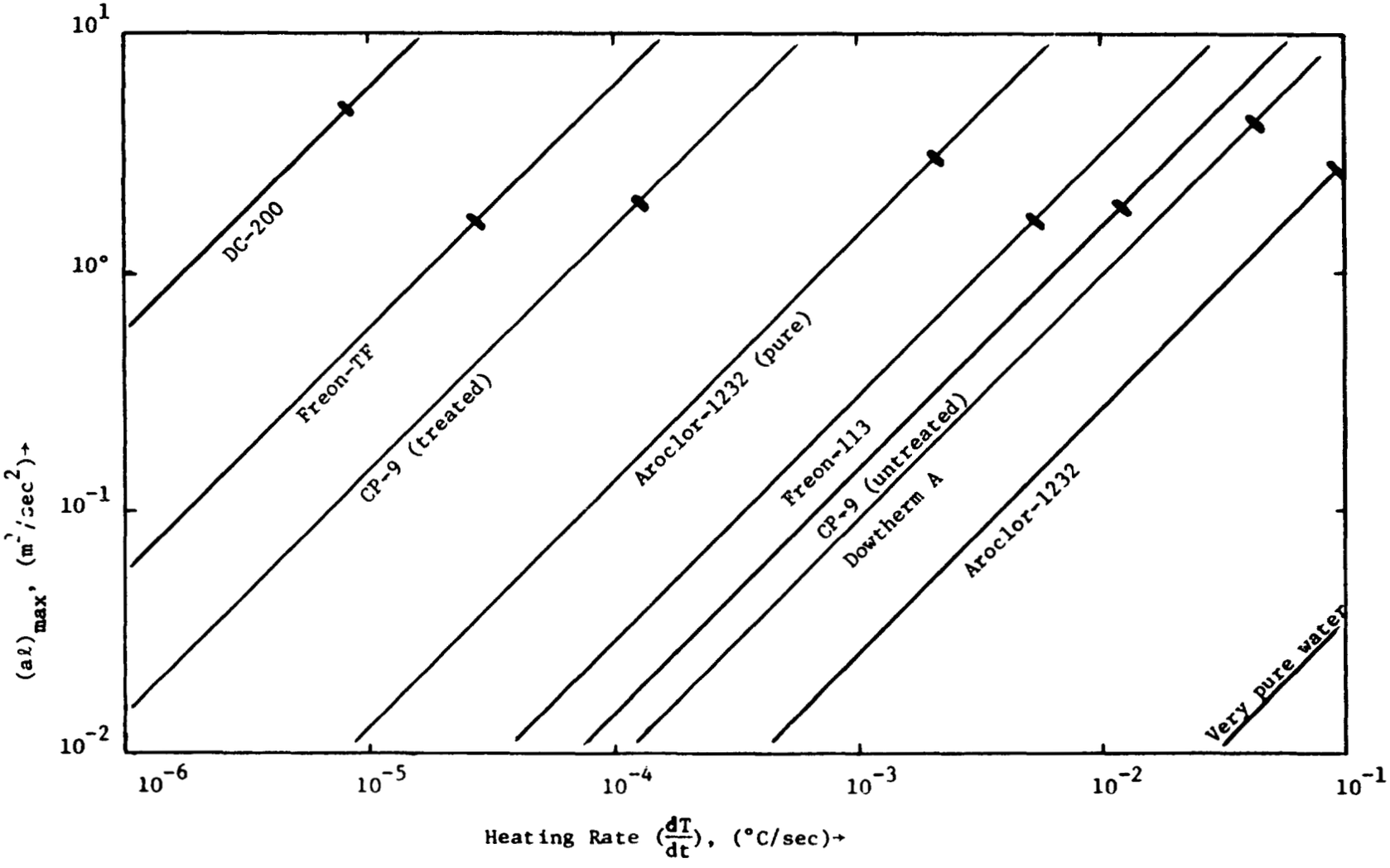

Figure 3.4 Electrohydrodynamic Static Orientation Performance Measure of Various Dielectric Liquids versus Instantaneous Joulean Heating Rate.

wave resonance, fluid can be lost by parametric excitation of large magnitude surface waves. The magnitude of these waves depends on fluid viscosity, and so the limitation on the sensitivity to vibrations of EHD containment is dependent on the fluid properties, the electric field strength, and the electrode structure itself. The problem is a very complex viscous fluid mechanics problem which has not yet admitted solution [25]. Thus, no general criterion for avoiding structure failure due to vibrations is in existence.

3. Cryogenic Liquid Orientation

Cryogenic liquids are nonohmic, highly insulating dielectrics, and thus it is natural to consider electrohydrodynamic orientation of these liquids in zero-gravity space processing applications. Because they are nonohmic, it is meaningless either to discuss joulean heating in cryogens or to attempt to represent cryogens in Figs. 3.3 or 3.4. The important limit is electrical breakdown in the liquid (or vapor). Thus, we use Eq. (3.5) with $E_o = E_b$, the breakdown strength of the vapor, to obtain $(a\ell)_{max}$. The Table 3.2 contains data for a number of important cryogens, including several isotopes of hydrogen. Unfortunately, the lack of vapor breakdown measurements at low vapor pressure for all but H_2 precludes a comprehensive set of calculations of $(a\ell)_{max}$.

Even without more complete data, it is possible to suggest that the electrohydrodynamic orientation and control of cryogens shows promise in zero-gravity space processing applications. Cryogenic liquids do not suffer from the problem of joulean heating, as do normal dielectrics, because they are excellent insulators. Controlling cryogens remotely by electric fields holds some clear advantages over mechanical systems in zero-gravity.

Table 3.2 Dielectric Properties of Certain Important Cryogenic Liquids and their Vapors (sources: [22,26])

Cryogenic Liquid	Relative Dielectric Constant $\varepsilon/\varepsilon_o$	Density ρ (kg/m^3)	Breakdown Strength (kV/cm) Liquid $E_{b\ell}$	Vapor E_{bv}	$(a\ell)_{max}$
N_2	1.454 (70°K)	$.808 \cdot 10^3$ (77.2°K)	~560 (77°K)	--	--
O_2	1.507 (80°K)	$1.14 \cdot 10^3$ (90°K)	--	--	--
He	1.055 (2.06°K)	$.147 \cdot 10^3$ (20.4°K)	~220 (4.2°K)	--	--
H_2	1.231 (20.4°K)	$.07 \cdot 10^3$ (20.4°K)	~1100. (14-20°K)	~280 (20°K)	--
D_2	1.26 (23.7°K)	$.16 \cdot 10^3$ (23.7°K)	--	--	--
DT	1.27 (24.4°K)	$.21 \cdot 10^3$ (24.4°K)	--	--	--
T_2	1.27 (25°K)	$.26 \cdot 10^3$ (25°K)	--	--	--

4. EHD Containers

Several concepts for electrohydrodynamic containers have been considered. The first is a simple electrode structure which may be fitted to the top of a liquid container to prevent loss of liquid from the container during temporary storage. See Figure 3.5a. The "bottle cap" would be disconnected from the high voltage when the container was to be emptied. This device would have a disadvantage in that evolved vapor would remain trapped as shown. Figure 3.5b shows a conceptualized container without this disadvantage. The electrode spacing varies from the bottom to the top, thus forcing out vapor bubbles This same structure could serve as a graduated cylinder useful in measuring out quantities of liquid. This latter concept is somewhat different from the "bottle cap" in that it relies on a uniform gradient in the electric field which is directed along the long axis of electrode structure. The behavior of such spatially varying structures has been studied in a pressurized environment (see Fig. 3.1c,d) and is well-understood. Refer to Appendix A.

B. Dynamic Liquid Orientation

Figure 3.6 illustrates a variety of electrode structures capable of containing and guiding dielectric liquids. Of these, the "tent" geometry has already been used in an electrohydrodynamic heat pipe [13] and the parallel-plate structure has been used in a dielectric siphon [27]. These electromechanical flow structures are not capable of pumping fluids, but if a body force or a pressure gradient is applied along the axis of the structure, liquid will flow. Attractive features of these flow structures include the extensive free surfaces which

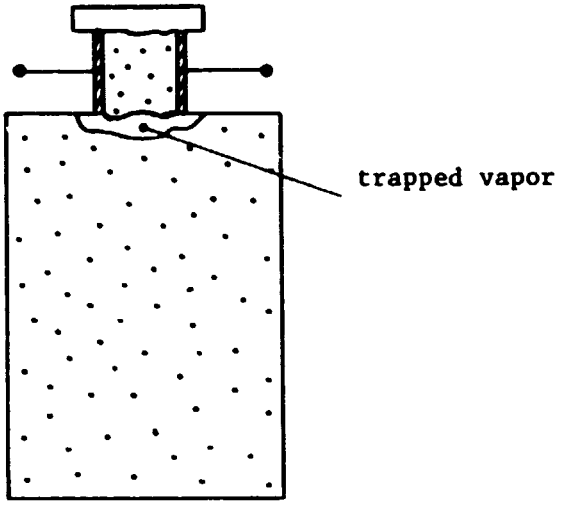

(a.) EHD "Bottle Cap" Concept

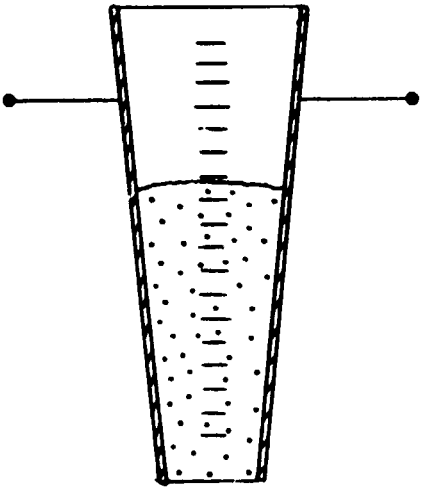

(b.) EHD Graduated Cylinder Concept

Figure 3.5 Various Electrohydrcdynamic Liquid Container Concepts.

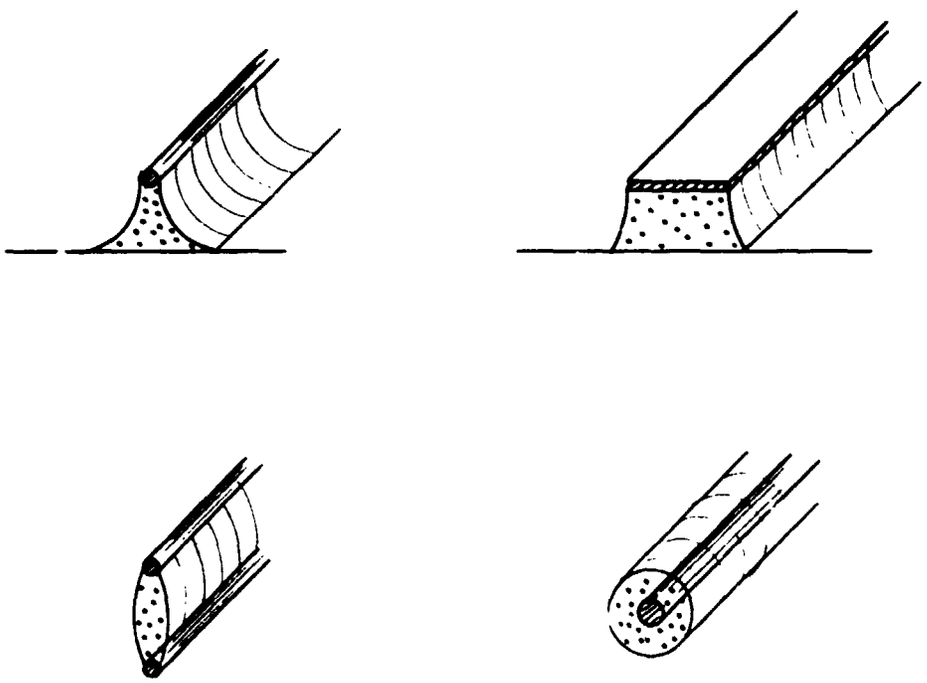

Figure 3.6 Various Electrohydrodynamic Flow Structures

permit collection of fluid at any point or evaporation and expulsion of vapor bubbles. Also, they can be controlled to an extent by varying the voltage. The chief limitation is the restriction to poorly conducting dielectrics.

1. Equilibrium and Stability

Electromechanical flow structures differ from static liquid orientation schemes primarily in that the net flow of liquid alters the dynamics and the equilibrium. The structures are normally stable with respect to small perturbations. These perturbations are manifested as electrohydrodynamically coupled surface waves, which are discussed elsewhere [28] and are of no interest here. The dynamic equilibrium is established by a balance of hydrodynamic, viscous, and body (acceleration) forces with the electrohydrodynamic surface force $(-\frac{1}{2} E^2 \nabla \epsilon)$.

2. Hydrodynamic Failure of EHD Flow Structures

If the hydrodynamic forces in an electromechanical flow structure are excessive, a pressure drop will exist along the structure which the electric field cannot support. Depending on the nature of the flow system, either unwanted fluid expulsion or "pinch-in" can occur. It is important to be able to avoid such failure.

Without specifying the geometry of the flow structure or the nature of the flow, it is still possible to specify the maximum allowed pressure drop $\Delta p_{max}(\dot{m}, \mu, \rho)$ before flow structure failure occurs.

$$\Delta p_{max}(\dot{m},\mu,\rho) \simeq \frac{(\epsilon - \epsilon_o)E_o^2}{2} \qquad (3.12)$$

where $\dot{m}$ = mass flow rate, μ = dynamic viscosity, ρ = fluid density, and E is the tangential electric field at the point where failure is about to occur. Equation (3.12) may be rewritten as shown below to show limits on Δp_{max} by electrical breakdown and joulean heating.

$$\Delta p_{max} \simeq \frac{(\varepsilon - \varepsilon_c)}{2\sigma} P_{diss} \qquad (3.13)$$

Equation (3.13) is plotted in Fig. 3.7 for a variety of dielectric fluids. To obtain the maximum flow rate $\dot{m}_{max}$ for a given geometry and electric field, $\Delta p_{max}(\dot{m},\mu,\rho)$ must be known.

C. Conclusions

A number of conclusions about electrohydrodynamic liquid handling and control can be gleaned from the above discussion. Some of these conclusions are quite general in their implications, but all are relevant to space processing applications.

- Liquid handling with electric fields is limited to non-conductors, such as dielectric insulators. Other liquids such as alcohol, water, etc. suffer unacceptably high joulean heating when strong electric fields are applied. Good conducting liquids are completely out of the range of possibility.

- Subject to realization of complex electrode configurations, dielectric fluids can be statically oriented in a variety of shapes and profiles. This capability may have interesting potential in the shaping and molding of plastic parts. Thorough assessment of this concept has been prevented by a lack of availability of electric properties for plastics in their molten states.

- Using EHD conduits of fairly simple design, dielectric liquids can be siphoned or transferred from one location to another. These structures are of interest because they are voltage-controlled and because they feature free liquid surfaces which are capable of ingesting liquid or expelling vapor. Such a flow structure might find application in a zero-gravity process which requires a controlled flow of a cryogenic liquid for cooling or processing.

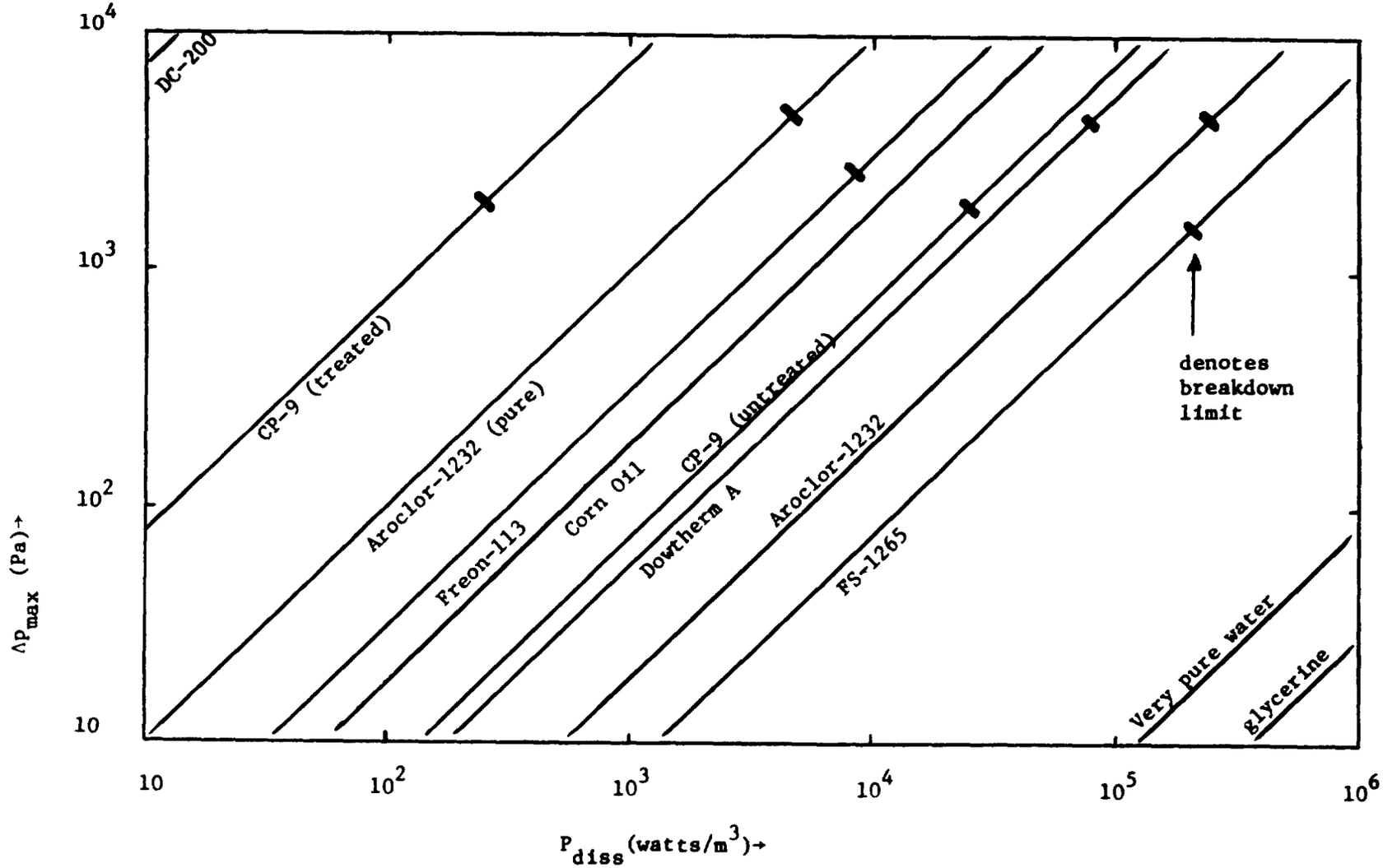

Figure 3.7 Maximum Sustainable Pressure Drop in EHD Flow Structure versus Joulean Power Dissipation for Various Dielectrics. (Breakdown Limit shown).

- Zero-gravity cryogenic liquid management in general may benefit from EHD liquid handling and control concepts discussed above. Cryogenic liquids have excellent dielectric properties, and apparently would not be subject to joulean heating limits with carefully prepared and polished electrodes.

- EHD liquid containers and measuring devices show some limited promise, but the requirement of high voltage, the limitation to insulating dielectrics, and the weight and cost penalties of such elaborate schemes may preclude their application.

IV. ELECTROSTATIC EXTRUSION

Containerless processing of various materials in their molten states is an area receiving much attention in the space processing technology program. The zero-gravity environment of a spacecraft, coupled with a means to levitate melts of certain materials, provides a possible method to process reactive and corrosive materials into useful forms. These materials include liquid metals and alloys, molten inorganic compounds, optical glasses, etc. One very interesting application of containerless processing is in the production of fine filaments of boron or other materials.

Experiments by Melcher and Warren [29] suggest the possibility that an electrostatic extrusion technique relevant to containerless, zero-gravity processing might be possible. The essence of their experiment is shown in Figure 4.1. A semi-insulating liquid (a water-glycerine mixture was used) is allowed to dribble from a small tube. By passing an electric current through the jet and applying an external electric field, the liquid jet can be stabilized, accelerated, and drawn into a very fine filament. Melcher and Warren's theoretical model of the dynamics of this current-driven jet successfully predicts the steady dynamical behavior. Relevant liquid parameters in the dynamical theory include dielectric constant, electrical conductivity, surface tension, liquid density, and at least an estimate of the viscosity.

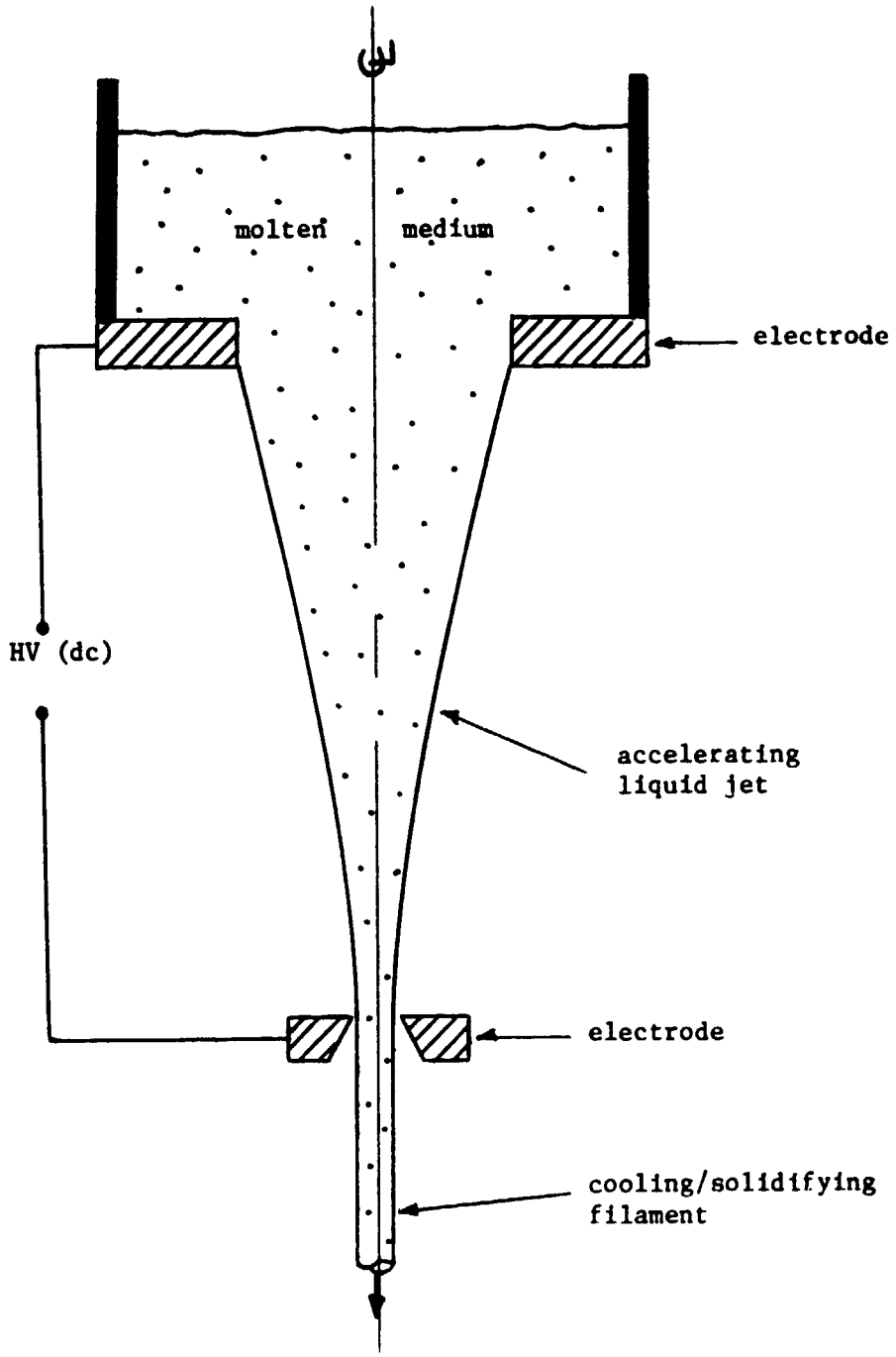

Figure 4.1 The Basic Electrostatic Extrusion Concept.

The proposed application of the current-driven jet to electrostatic extrusion of molten materials is complicated by several factors, including a heat transfer problem associated with solidification of the thin, convecting, EHD-stabilized molten jet, and the temperature-dependent nature of various fluid properties. It is quite likely that the transfer of heat away from the flowing jet to induce solidification can be promoted by using a corona-wind cooling mechanism discovered by Blomgren [30]. However, the temperature-dependent property problem is difficult to assess without theoretical modeling efforts beyond those of Melcher and Warren. This point illustrates the need for good thermophysical property data in addition to the properties previously mentioned, over reasonable temperature ranges. Such data was not found to be available in this study. As a result, no substantial progress in modeling the behavior of a convecting, solidifying current-driven jet was made.

On the experimental front, some effort was devoted to the study of the water-glycerine current-driven jet, in an effort to reproduce the sub-critical, accelerating jet condition [27]. Sulfur received some consideration as a molten medium because of its relatively low melting point and its insulating properties in the solid state. However, numerous practical complexities appeared to preclude completion of any meaningful experiments in the one-year time period of this study.

Without experimental demonstration of electrostatic extrusion or feasibility calculations based on theoretical models, it is not possible to assess the potential of this concept in space processing.

The difficulties with obtaining property data for the molten states of various materials suggest that an experimental approach, possibly using molten sulfur, would be appropriate.

V. ELECTROHYDRODYNAMIC EFFECTS ON CRYSTAL GROWTH

The work performed on this task consists of a literature review prepared by D. R. Winder [31]. Numerous effects of electric fields on crystal growth processes have been identified, but few if any have been investigated. The implication of these effects for a zero-gravity environment are unknown. The lack of electrical properties data on the molten states of crystal-producing materials, previously mentioned with regard to bubble purging (§ II.C.4) and electrostatic extrusion (§ IV), precluded an in-depth survey of the potentialities. For completeness, the references listed below, compiled by D. R. Winder, are provided. The subject headings under which they appear provide a measurement of the range of electric field and electrohydrodynamic effects relevant to crystallography.

A REVIEW OF THE LITERATURE ON THE EFFECTS OF ELECTRIC FIELDS ON CRYSTAL GROWTH

(compiled by D. R. Winder, July, 1974)

1. Crystal growth directly controlled by electric fields

1.1 Whiskers.

Bacon, R., "The Structure and Elastic Properties of Graphite Whiskers," Bull. Am. Phys. Soc., Sec. II, 2, 131 (1957), and other places. Scroll-like whiskers are imbedded in boule formed by a direct current carbon arc.

Bienfait, M., and Kern, R., "Forme D'Equilibre d'un Cristal en Microscopie par Emission de Champ," in Crystal Growth: Proc. Intl. Conf. on Crystal Growth, H. S. Peiser, ed., Boston: 1957, Pergamon Press.

Carroll, R. W., and Schubert, C. C., "Field Evaporation of a Screw Dislocation in Tungsten," J. Appl. Phys. 39, 2339 (1968).

Gomer, R., "Some Observations on Field Emission from Mercury Whiskers," in Growth and Perfection of Crystals, Doremus, et. al., ed., 1958, Wiley.

Nosov, A. A., et.al; "Action of an Electric Field on the Formation of Gold Whisker Single Crystals," Radiotech. Elektron. 17, 366 (1972), from Chem. Abs. 76 #132463.

1.2 Shape Control.

Gaule, G., Kedesdy, H. H., and Rouge., L. J. D., U. S. Patent 3,096,158; July 2, 1963.

1.3 Nucleation and Condensation.

Cisse, J., and Bolling, G. F., "Electro-Nucleation of Undercooled Salol, J. Cryst. Growth 7, 37 (1970).

Dove, D. B., "Possible Influence of Electric Charge Effects on the Initial Growth Processes Occurring During Vapor Deposition of Metal Films onto Substrates inside the Electron Microscope," J. Appl. Phys. 35, 2785 (1964).

Fletcher, N. H., The Physics of Rainclouds, Cambridge Univ. Press (1962).

Hirth, J. R., and Pound, G. M., "Condensation and Evaporation," Prog. Mat. Sci. 11 (1963), the Macmillan Co., N. Y. (1963).

Kaschiev, D., "Nucleation in External Electric Field," J. Cryst. Growth 13/14, 128 (1972).

Murayama, Y., "Effects of Electric Field on the Orientation and Particle Arrangement of Gold Deposits Evaporated in Vacuo," Thin Solid Films 12, 287 (1972).

Pruppacher, H. R., "The Effects of Electric Fields on Cloud Physical Processes," Z. Angew. Math. Phys. 14, 490 (1963).

Russell, K. C., "Nucleation on Gaseous Ions," J. Chem. Phys. 50, 1809 (1969).

Wilson, C. T. R., Phil. Trans. Roy. Soc. (Lon) 192, 403 (1899) and several others.

1.4 Crystallization in an Electric Field.

Asano, Y., Suzuki, T., "Effect of Crystallization in Polyethylene Terephthalate Electrets," J. Appl. Phys. 44, 1378 (1973).

Bartlett, J. T., Vanden Heuval, A., and Mason, B. J., "The Growth of Ice Crystals in an Electric Field," Z. Angew. Math. Phys. 14, 599 (1963).

Belan, S. A., Boletov, I. E., and Komarova, L. I., "Effect of Electric Field on Crystallization of Amorphous Selene," Izvestiya Vysshikh Ochebnykh Zavedenii Fizika, 106 (1971), from Sci. Cit. 1971.

Camp, P. R., and Barter, F. C., "An Electrical Effect on the Growth of Ice Crystals," Nature 200, 350 (1963).

Crowther, A. G., "Preliminary Investigation into the Growth of Ice Crystals from the Vapour in an Electric Field in the Temperature Range -11 to -15°C., "J. Cryst. Growth 13/14, 241 (1972).

Hanani, M., "Crystallization of Rochelle Salts in Electric Field," J. Appl. Phys. 92, 206 (1971).

Nassau, K., and Levinstein, H. D., "Ferroelectric Behavior of Lithium Niobate," Appl. Phys. Letter 7, 69(1965).

Lichten, M., Witt, A. F., and Gatos, H. C., "Modulation of Dopant Segregation by Electric Currents in Czochralski-type Crystal Growth," J. Electrochem. Soc. 118, 1013 (1971).

Melcher, D., "Experimentelle Untersuchung von Vereisungserscheinungen," Z. Angew. Math. Phys. 2, 421 (1951).

Motoc, C., "An Electric Field Influence on Dendritic Growth," J. Cryst. Growth 12, 309 (1972).

Abdullaev, G. B., Lange, V. N., Mamedov, K. P., and Odobesku, A. I., "Effect of an Electrical Field on the Crystallization of Selenium," Fiz. Khim. Obrab. Mater. (3) 151-3, from Chem. Abs. 77-93834.

Geller, I. Kh., Kolomiets, B. T., and Popov, A. I., "Crystallization of Selenium under the Action of an Electrical Field of Varying Frequency," Izv. Akad. Nauk. SSSR, Neorg. Mater 1973, 9 (1) 127, from Chem. Abs. 78, 102807.

Ladinska, S. I., Agranat, A. L. and Sulzdkii, F. T., "Electric Field Effect on Phytosterol Crystallization from Sulfate Soap Alcohol-Water Solution," Zhurnal Prikiadnoi Knimic, 43, 1091 (1970), from Sci. Cit., 1970.

Mikhaylo, V. A., Korniyev, M. V. and Vertopra, V. N., "Crystallization of Bismuth and Tin from Melt in Liquid Gallium in an Electric Field," Physics of Metals and Metallography USSR, 28, 196 (1969), from Sci. Cit., 1970.

Schieber, M., Hanani, M., and Eidelberg, J., "Crystallization in Magnetic and Electrical Fields," U. S. Nat. Tech. Inform. Serv. AD Rep. 1972 No. 751204, (NTIS: Govt. Rep. Announce.)(US) 1973, 73 (1), 2150, from Chem. Abs. 78, (1973) 102822.

1.5 Plasmas.

Blachman, A. G., "D C Bias-sputtered Aluminum Films," J. Vac. Sci. Tech. 10, 299 (1973).

Fagen, E. A., Nowicki, R. S., and Seguin, R. W., "Effects of D C Substrate Bias on the Properties of r. f.-Sputtered Amorphous Germanium Ditelluride Films," J. Appl. Phys. 45, 50 (1974).

Kawabuchi, K., and Magari, S., "UO_2 Deposition from its Plasma," Appl. Phys. Lett. 22, 336 (1973).

Mattox, D. M., "Fundamentals of Ionplating," J. Vac. Sci. Tech. 10, 47 (1973).

Uemura, Y., Tanaka, D., and Iwata, M., "Some Properties of Thin Aluminum Nitride Films Formed in a Glow Discharge," Thin Solid Films 20, 11 (1974).

2. Heating Control by Electric Fields

2.1 Joule Heating and Convection.

Carruthers, J. R., "Thermal Convection Instabilities Relevant to Crystal Growth from Liquids," in Preparation and Prop. Sol. St. Materials 2, 1974. Section 5-c treats the effects of electric fields.

Turnbull, R. J., "Free Convection from a Heated Vertical Plate in a Direct-Current Electric Field," Phys. Fluids 12, 2255 (1969). This includes a survey of previous work with 24 references.

Gross, M. J., and Porter, J. E., "Electrically Induced Convection in Dielectric Liquids," Nature 212, 1343 (1966).

Lykoudis, P. S., and Yu, C. P., "The Influence of Electrostrictive Forces in Natural Thermal Convection," Int. J. Heat Mass Transfer 6, 853 (1963).

Roberts, P. H., "Convection in Horizontal Layers with Internal Heat Generation--Theory," J. Fluid Mech. 30, 33 (1967).

Roberts, P. H., "Electrohydrodynamic Convection," Quart. J. Mech. Appl. Math. 22, 211 (1969).

Schwiderski, E. W., and Schwab, H. J. A., "Convection Experiments with Electrolytically Heated Fluid Layers," J. Fluid Mech. 48, 703 (1971).

Sparrow, E. M., Goldstein, R. J., and Jonsson, V. K., "Thermal Instability in a Horizontal Fluid Layer: Effect of Boundary Conditions and Non-Linear Temperature Profile," J. Fluid Mech. 18, 513 (1964).

Tritton, D. J., and Zarraga, M. N., "Convection in Horizontal Layers with Internal Heat Generation Experiments," J. Fluid Mech. 30, 21 (1967).

2.2 Body Forces.

Ahsmann, G., and Kronig, R., "The Influence of Electric Fields on the Convective Heat Transfer in Liquids," Appl. Sci. Res. A2, 235 (1950).

DeHaan, M. J., "The Influence of Electric Fields on the Convective Heat Transfer in Liquids II," Appl. Sci. Res. A3, 83 (1931).

Kronig, R., and Schwarz, N., "On the Theory of Heat Transfer from a Wire in an Electric Field," Appl. Sci. Res. A1, 35 (1947).

Turnbull, R. J., "Electroconvective Instability with a Stabilizing Temperature Gradient. I. Theory. II. Experimental Results," Phys. Fluids, 11, 2588, 2597 (1968).

Turnbull, R. J., "Effect of a Non-Uniform Alternating Electric Field on the Thermal Boundary Layer Near a Heated Vertical Plate," J. Fluid Mech. 49, 693 (1971).

Wong, J., and Melcher, J. R., "Thermally Induced Electroconvection," Phys. Fluids 12, 2264 (1969).

3. Electrochemistry

3.1 General.

Nabarro, F. R. N., and Jackson, P. J., "Growth of Crystal Whiskers," in Growth and Perfection of Crystals, Doremus, et.al., ed., Wiley, 1958.

3.2 Electrodeposition.

Barton, J. L., and Bockris, J. O'M., "The Electrolytic Growth of Dendrites from Ionic Solution," Proc. Roy. Soc., A268, 485 (1962).

Corish, J., and OBriain, C. D., "The Growth and Dissolution of Silver Whiskers," J. Cryst. Growth 13/14, 62 (1972).

Hamilton, D. R., "Dendritic Growth in Electrolytes," Bull. A. P. S. 8, 227 (1963).

Liaw, H. M., and Faust, Jr., J. W., "Effect of Growth Parameters on Habit and Morphology of Electrodeposited Lead Deposits," J. Cryst. Growth 18, 250 (1973).

Price, P. B., Vermilyea, D. A., and Webb, M. B., "On the Growth and Properties of Electrolytic Whiskers," Acta Met. 6, 524 (1958).

Reddy, T. B., "Surface Diffusion Processes and Dendritic Growth in the Electrodeposition of Ag from Molten Halides," J. Electrochem. Soc. 113, 117 (1966).

3.3 Interfacial Phenomena.

Bikerman, J. J., Physical Surfaces, New York, Academic Press, 1970.

Davies, J. T., and Rideal, E. K., Interfacial Phenomena, 2nd ed., New York, Academic Press, 1963.

VI. ELECTROHYDRODYNAMICALLY CONTROLLED MIXING

Late in the conduct of this research program, attention was directed to the work of J. F. Hoburg, a doctoral student in the Department of Electrical Engineering at the Massachusetts Institute of Technology. Hoburg's thesis topic is electrohydrodynamic mixing processes. The use of electrohydrodynamic mixing mechanisms in zero-gravity space processing was alluded to in the original proposal, but was not considered part of the research program. However, exposure to Hoburg's work on the subject prompted the principal investigator to add a brief review of electrohydrodynamic mixing to the final report.

A. Introduction

Mixing operations are of fundamental significance in numerous proposed zero-gravity space processing applications. Examples include the mixing of various miscible and/or immiscible compounds and substances to produce new alloys, composite materials, etc. The zero-gravity environment itself is attractive, because separation of immiscibles does not occur as rapidly as in a terrestrial gravitational field. For this reason, various mixing methods must be considered for their application in space processing.

Mixing may be characterized by two measures: <u>scale</u> and <u>intensity</u>. The <u>scale</u> is a measure of the average distance between centers of maximum property variations in a mixture. <u>Intensity</u> is a measure of the magnitude of property variation within a mixture. For purposes here, it is convenient to use the scale measure to compare various mixing mechanisms. The most common means of achieving mixing is

mechanical stirring. This process is quite effective at scales on the order of size of the mechanical stirrer itself. If finer scale mixture is required, then a stirrer with a more elaborate and smaller structure must be used. For this reason, a limit on the capabilities of mechanical stirring exists. This limit might be quantified in terms of the time required to achieve a mixture of a certain scale. The time required to achieve a mixture scale much smaller than the size of the stirrer becomes excessive.

Another mixing mechanism, diffusion, exists naturally in all mixtures. Diffusion can achieve mixing on very fine scales in very short times. However, because diffusion times depend on the square of the characteristic length, diffusion is too slow on larger scales.

Hoburg states that, for mixing scales intermediate between those of mechanical mixing and diffusion, electrohydrodynamic mixing may provide an attractive alternative [11]. For this reason, EHD mixing merits consideration for space and terrestrial processing applications.

B. Electrohydrodynamic Mixing

1. Important Mechanisms

To effect mixing of components using electric fields, a number of different mechanisms suggest themselves. Included are double-layer, ion-drag, and conductivity gradient phenomena. While only the latter mechanism is considered here, all three are similar dynamic body forces which tend to mix adjacent fluid parcels of differing properties. For example, an electric field applied to an ohmic conducting fluid with a conductivity profile will induce free charge in the fluid bulk, which is acted on by the electric field, producing motion. From thermodynamic considerations it is clear that the induced fluid motions will act to reduce the scale of inhomogeneities This is of course the desired result, namely mixing.

Two limiting cases of conductivity gradient situations may be identified. One is the weak gradient case of a heated liquid, a partially mixed combination of miscible liquids, or a solid dissolving in a liquid. Zahn has considered what he calls the "space-charge dynamics" of such situations [32]. The other limiting case is the strong gradient situation, which exists in the immediate vicinity of the interface between miscible or immiscible fluids. Hoburg has considered this latter category of problems [11].

Figures 6.1a and b show the simple configurations which can be used to achieve mixing using the electrohydrodynamic, conductivity-gradient mechanisms. In Figure 6.1a, an electric field is imposed tangentially to the interface between two liquids of differing conductivities. If an electric field is applied, the interface will start to distort and mixing will start almost immediately. Visual observation shows that the scale of the mixture begins to change very quickly. After a period of time inversely dependent on the applied electric field, a reasonably homogeneous mixture is achieved. Hoburg has obtained experimental evidence that the required mixing time is related to the electric-viscous time discussed in the next section.

Somewhat similar results are obtained for the case of an electric field applied perpendicular to the interface, as shown in Figure 6.1b. Most if not all of the experiments to date have been performed with miscible, insulating dielectric liquids and with electrolytes. Good mixing of conductivity-doped corn oil and of freon/corn oil mixtures has been observed. Apparently, no experiments have yet been performed with immiscible combinations.

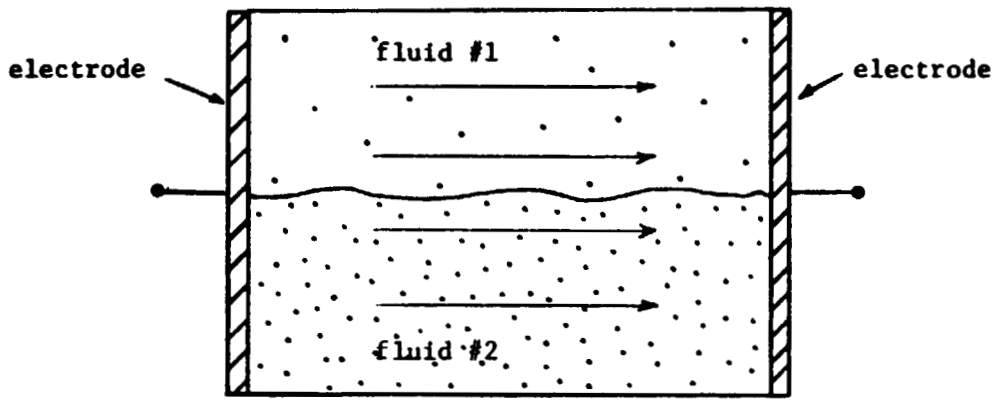

(a) Electric Field parallel to interface between liquids of differing conductivities.

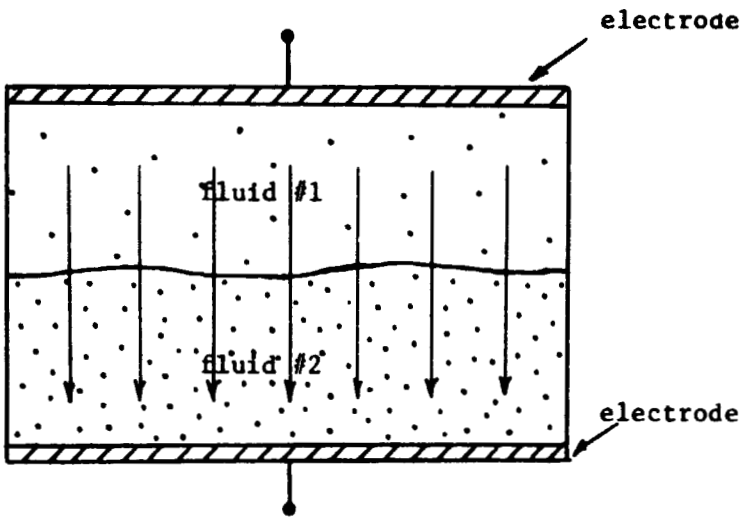

(b) Electric field perpendicular to interface between liquids of differing conductivities.

Figure 6.1 Two Fundamental Electrohydrodynamic Mixing Schemes.

3. The Electric-Viscous Time

Melcher has identified an electric-viscous characteristic time ($\tau_m = \mu/\varepsilon E^2$) which is a common modulus in many viscous dominated electrohydrodynamic problems [17]. Hoburg has recognized that this same time constant plays a crucial role in EHD mixing problems involving a conductivity gradient [11]. This quantity $\mu/\varepsilon E^2$ is best interpreted as the time required to effect substantial mixing of ohmic conductors on a scale comparable to the gradient. Note that τ_m is a strong inverse function of the electric field; thus, it is possible to control mixing rates through control of the applied voltage.

The electric-viscous time is useful in relative comparisons of the efficacy of EHD mixing of various liquid substances. It is convenient to relate τ_m to the joulean heating rate:

$$\tau_m = \frac{\mu}{\varepsilon E^2} = \left(\frac{\mu\sigma}{\varepsilon}\right)(\sigma E^2)^{-1},$$

$$= \left(\frac{\mu\sigma}{\varepsilon}\right) P_{diss}^{-1} \qquad (6.1)$$

Figure 6.2 plots τ_m versus P_{diss} for a number of fluids. The figure shows that electrohydrodynamic mixing is not limited to insulating dielectric liquids, but includes some moderate conductors such as methyl alcohol and water. Further, some mixing processes may tolerate or even benefit from some joulean heating. It is clear, however, that EHD mixing of good conductors (liquid metals, etc.) is not likely to be effective due to completely unacceptable joulean heating levels.

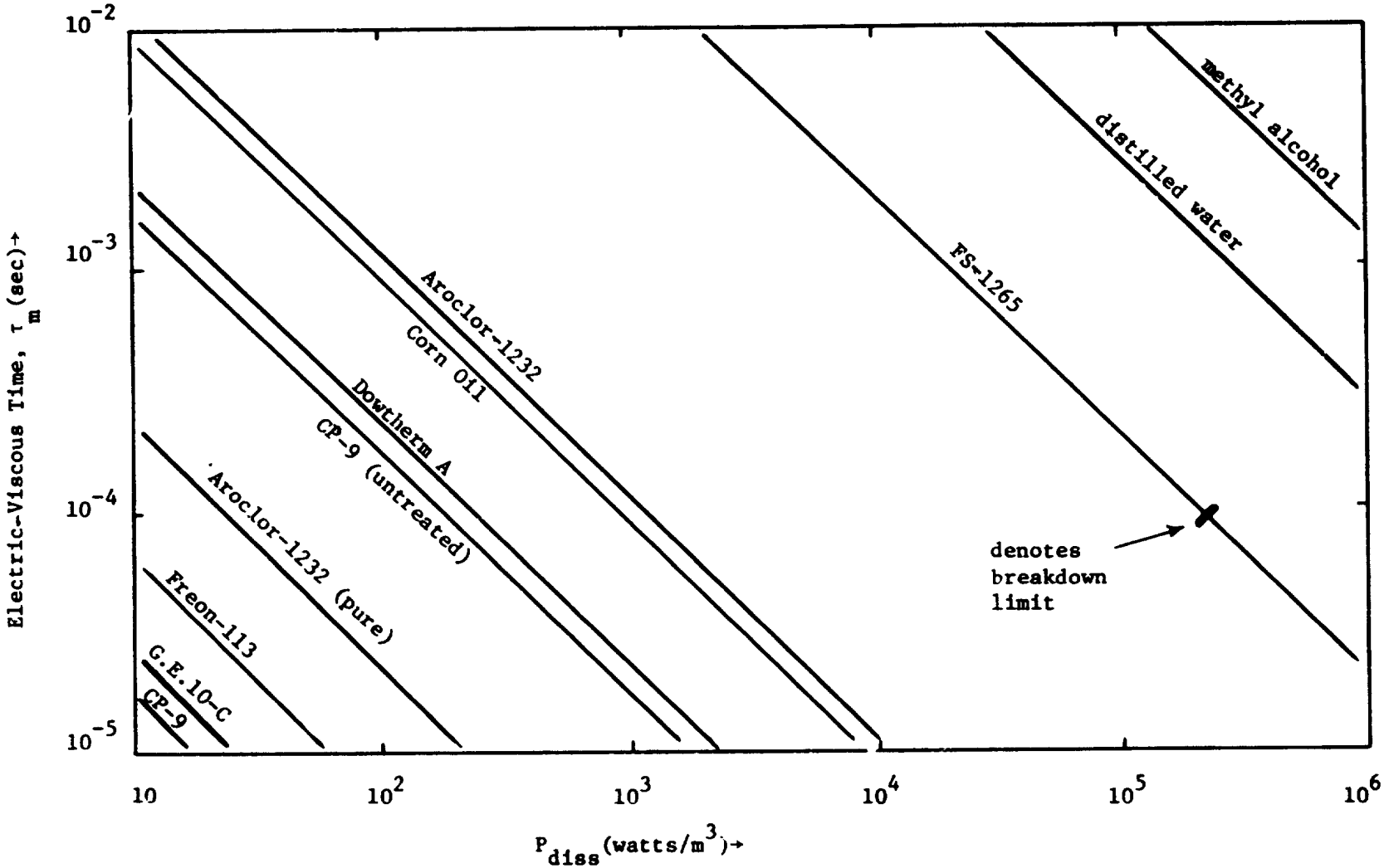

Figure 6.2 Electric-Viscous Mixing Time for Various Dielectric Liquids versus Joulean Power Dissipation.

C. Conclusions

1. Discussion

Two potential applications of electrohydrodynamic mixing appear promising in space processing. These are (i) the intermediate scale mixing of miscible substances (or possibly the promotion of dissolution of solids in liquids, and (ii) the mixing of immiscible substances to form alloys and composites. A hindrance to thorough assessment of the latter application is the lack of appropriate properties of relevant materials in their liquid states. Another problem is the fact that no experimental attempt to mix immiscibles has been reported.

Several general conclusions can be made in summary of the foregoing discussion of this chapter.

- Electrohydrodynamic mixing is effective on mixing scales intermediate between those of mechanical stirring (large scale) and diffusion (small scale).
- EHD mixing is characterized by the electric-viscous time, which is proportional to the inverse of the square of the electric field. Mixing rates may thus be controlled by varying the applied electric field.
- EHD mixing is practically limited to liquids with moderate or poor conductivity. Electrolytic solutions are probably acceptable, but highly conducting substances such as liquid metals are not.

2. Proposed Future Work

Reger [33] has identified a class of immiscible crystalline organic couples which are of interest in space processing, due to their potentially attractive optical properties. He also mentions the value of mixtures of certain insulating and semi-insulating materials. The immiscible crystalline organics appear well-suited to mixing using electric fields in a zero-gravity environment, because the proposed application of these couples, Christiansen IR filters, requires fairly precise control of the mixture scale. An experimental program aimed at studying electrohydrodynamic mixing of certain immiscible couples is presently being proposed.

VII. SUMMARY AND CONCLUSION

In this chapter, the results of this study of electrohydrodynamic space processing are presented in summary form. Based on these results, conclusions are drawn about the potential value of various EHD space processing concepts. Identification is made of cases where more basic experimental research is called form.

A. General Discussion

The purpose of this research program has been to investigate the effects and applications of electrohydrodynamic phenomena on space processing. The approach has included experimental work and theoretical calculations, performed to test the feasibility of various concepts. Some of the experiments required the simulation of a zero- or low-gravity environment. This was achieved by the use of a high pressure vessel, which was designed and constructed during the course of this research program. Appendix B contains a description of this facility.

A serious limitation of this study is the lack of data on materials in the molten state. Such electrical properties as dielectric constant, conductivity, and breakdown strength, and mechanical properties, such as viscosity, etc., are necessary to a proper evaluation of proposed electrohydrodynamic space processing concepts. For molten materials, e.g., plastics, such properties are apparently non-existent. This is unfortunate because EHD effects might be very useful in the handling and control of plastics. Without this data, it is not possible to draw firm conclusions about the zero-gravity processing of plastics using electrical fields. Still, the theoretical calculations are presented in such a way that new materials can be easily evaluated for their potential application, once the appropriate properties are known.

B. Specific Conclusions

1. Dielectrophoretic Unit Separation and Bubble Positioning

- Liquid-gas separation shows promise in applications related to bubble purging in melts and bubble control in cryogenics.

- Liquid-liquid separation does not appear to be workable, because the liquid bubbles distort significantly when strong electric fields are applied.

- Liquid-solid separation is a promising means to separate small particles of dielectric material out of another liquid dielectric, though quite strong electric fields are required, due to the normally very small difference in dielectric constants for the liquid and solid.

- Dielectrophoretic bubble positioning and control has potential applications in laser fusion target production, cryogenics, and optical devices.

- Dielectrophoresis is strictly limited to insulating dielectric liquids by joulean heating, which produces excessive heating in semi-insulating liquids such as water or methyl alcohol.

- Dielectrophoresis can be hampered by electroconvection if dc electric fields are used. For ac fields the effect is not apparent.

- Diffusion effects limit the lower size of particles or bubbles to > 1μm; an upper limit on vapor bubble size is imposed by bubble distortion.

2. Electrohydrodynamic Liquid Handling

- The static control of insulating polarizable liquids such as organic dielectrics or cryogenics has been demonstrated. Possible applications include liquid containers and measures, plus molding of molten media.

- The dynamic control of insulating polarizable liquids in siphons and other electrohydrodynamic flow structures has potential application in the control of coolants and cryogenics in zero-gravity.

- Because strong electric fields are required, fluids oriented by polarization forces are subject to joulean heating, and this heating is excessive in all but the insulating dielectric liquids. Such liquids as water cannot be oriented statically or dynamically by these means.

- Electrical breakdown of the vapor or liquid is another significant limit on the static or dynamic orientation of dielectric liquids with electric fields.

- Other problems include charge relaxation, which limits the use of dc electric fields, and surface resonances, which limit useable electric field frequencies and require precautions regarding mechanical vibrations.

3. Electrostatic Extrusion

   - Electrostatic extrusion of continuous solid filaments of material from molten fluid masses has been proposed but not yet demonstrated experimentally, due to the difficulty in finding suitable materials with low melting points and moderate conductivities.

   - Feasibility considerations were severely hampered by the lack of material properties data for substances in their molten states.

   - Electrostatic extrusion is one area of electrohydrodynamic space processing where the electrical conductivity limitation should not be too severe.

4. Electrohydrodynamic Effects on Crystal Growth

   - A literature search into the effects of electric fields on crystal growth uncovered several effects which might be of interest in zero-gravity crystallography.

5. Electrohydrodynamically Controlled Mixing

   - EHD mixing of inhomogeneous mixtures can be effective on scales intermediate between those of diffusion and mechanical stirring.

   - Application possibilities include the mixing of immiscible couples and composite materials, mixing of reactive components in chemical processes, promotion of dissolution of solids in liquids.

   - Joulean heating limits the mixing components to insulating and semi-insulating liquids (probably including aqueous mixtures).

   - Key experiments with immiscible couples have to be performed to determine the real efficacy of electrohydrodynamic mixing of certain potentially practical substances.

C. Future Work Recommendations

1. Molten media properties acquisition

It would be very beneficial to any future assessment of the electrohydrodynamic effects and their application to space processing if a data bank on the properties of a wide range of materials could be compiled. For example, the electrical conductivity and dielectric constant of molten plastics would have been very useful. Other properties such as viscosity, surface tension, etc., would also be useful.

2. Electrostatic Extrusion

The interest in producing continuous filaments of boron, or other materials, is strong enough that the effort might be put into a demonstration experiment with a more easily handled substance. Sulfur has a relatively low melting point, and its electrical conductivity in the molten state is probably in the correct range, so that it might be chosen for this demonstration experiment.

3. Electrohydrodynamic Mixing of Immiscibles

The identification of a class of immiscible crystalline organic couples which might have interesting applications in IR filters [31] prompts the recommendation that EHD mixing mechanisms be considered in greater detail than has been achieved in the present study. As discussed in Chapter VI, EHD mixing is controllable through the electric field strength. This capability may be important in preparation of Christiansen type IR filters, which consist of immiscible materials mixed on a scale roughly equal to the wavelength of the desired IR transmission spectrum.

References

1. Koval, L. F., and Bhuta, P. G., "Slosh Control by Dielectrophoresis," Proceedings, Institute of Environmental Sciences, San Diego, 1966, pp. 237-242.

2. Melcher, J. R., Guttman, D. S., and Hurwitz, M., "Dielectrophoretic Orientation," J. Spacecraft and Rockets, Vol. 6, January, 1969, pp. 25-32.

3. Melcher, J. R., Hurwitz, M., Fax, R. G., "Dielectrophoretic Liquid Expulsion," J. Spacecraft and Rockets, Vol. 6, September, 1969, pp. 961-967.

4. Lubin, B. T. and Hurwitz, M., "Vapor Pullthrough at a Tank Drain with and without Dielectrophoretic Baffling," Proc. of Conference on Long-Term Cryo-Propellant Storage in Space, NASA/Marshall Space Flight Center, Huntsville, Ala., October, 1966.

5. Choi, H. Y-H., "Electrohydrodynamic Boiling Heat Transfer," Ph.D. Thesis, Department of Mechanical Engineering, Massachusetts Institute of Technology, Cambridge, Mass., January, 1962.

6. Johnson, R. L., "Effect of an Electric Field on Boiling Heat Transfer," AIAA Journal, Vol. 6, August, 1966, pp. 1456-1460.

7. Jones, T. B., and Schaeffer, R. C.,"Electrohydrodynamically Coupled Minimum Film Boiling in Dielectric Liquids," to be presented at 10th AIAA Thermophysics Conf., Denver, Colo., May, 1975.

8. Choi, H. Y-H., "Electrohydrodynamic Condensation Heat Transfer," Trans. ASME - J. Heat Transfer, Vol. 90-C, February, 1968, pp. 1-5.

9. Stuetzer, O. M., "Ion-Drag Pressure Generation," J. Applied Phys., Vol. 30, July, 1959, pp. 984-994.

10. Ochs, H. T., "Traveling-Wave Electrohydrodynamic Pumping," M. S. Thesis, Department of Electrical Engineering, Massachusetts Institute of Technology, 1967.

11. Hoburg, J. F., "Electrohydrodynamic Mixing," Ph.D. Thesis, Department of Electrical Engineering, Massachusetts Institute of Technology, in preparation.

12. Jones, T. B., "An Electrohydrodynamic Heat Pipe," Mechanical Engineering (ASME), Vol. 96, January, 1974, pp. 27-32.

13. Jones, T. B., and Perry, M. P., "Electrohydrodynamic Heat Pipe Experiments," J. Applied Phys., Vol. 45, May, 1974, pp. 2129-2132.

14. Holmes, R. Z., and Anno, J. N., "An Electrofluid-Dynamic Cooling System Concept for Spacecraft Environmental Control," ASME paper #70-HT/SpT-24, presented at Space Technology and Heat Transfer Conf., Los Angeles, Cal., June, 1970.

15. Reynolds, J. M., et al., "Design Study of a Liquid O_2 Converter for Use in a Weightless Environment," TDR-63-42, AMRL, Wright-Patterson AFB, Ohio, 1963.

16. Pohl, H. A., "The Motion and Precipitation of Suspensoids in Divergent Electric Fields," J. Applied Phys., Vol. 22, July, 1951, pp. 869-871.

17. Melcher, J. R., "Electrohydrodynamics," Applied Mechanics, Proc. of Thirteenth International Congress of Theoretical and Applied Mechanics, Moscow, August, 1972.

18. McCreight, L. R., and Griffin, R. N., "Unit Separation Processes in Space," presented at Space Processing and Manufacturing Meeting, NASA/ Marshall Space Flight Center, Huntsville, Ala., October, 1969, pp. 216-237.

19. Bliss, G., "Electric Field Effects on Bubbles in Dielectric Liquids",M.S. Thesis, Department of Electrical Engineering, Colorado State University, in preparation.

20. Harper, J. F., "The Motion of Bubbles and Drops Through Liquids," in Advances in Applied Mechanics, Academic Press, N. Y., 1972, pp. 59-129.

21. Garton, C. G., and Krasucki, Z., "Bubbles in Insulating Liquids: Stability in an Electric Field," Proc. Royal Soc. (London), Vol. A280, 1964, pp. 211-226.

22. Roder, H. M., et al., "Survey of the Properties of the Hydrogen Isotopes Below their Critical Temperatures," NBS Technical Note #641, August, 1973.

23. Jones, T. B., "Dynamics of Electromechanical Flow Structures," Ph.D. Thesis, Department of Electrical Engineering, Massachusetts Institute of Technology, August, 1970.

24. Melcher, J. R. and Schwartz, W. J., "Interfacial Relaxation Overstability in a Tangential Electric Field," Phys. Fluids, Vol. 11, December, 1968, pp. 2604-2616.

25. Jones, T. B., "The Interfacial Parametric Electrohydrodynamics of Insulating Dielectric Liquids," J. Applied Phys., Vol. 43, November, 1972, pp. 4400-4404.

26. Handbook of Chemistry and Physics, C. D. Hodgman, ed., Chemical Rubber Publishing Co., 41st edition, 1959.

27. Jones, T. B., Perry, M. P., and Melcher, J. R., "Dielectric Siphons," Science, Vol. 174, 17 December, 1971, pp. 1232-3.

28. Jones, T. B., and Melcher, J. R., "Dynamics of Electromechanical Flow Structures," Phys. Fluids, Vol. 16, March, 1973, pp. 393-400.

29. Melcher, J. R., and Warren, E. P., "Electrohydrodynamics of a Current-carrying Semi-insulating Jet," J. Fluid Mech., Vol. 47, 1971, pp. 127-143.

30. See J. Fisk, Ham Radio, Vol. 5, January, 1972, p. 4 for a discussion of O. Blomgren's work on corona wind cooling.

31. Winder, D. R., "Effects of Electric Fields on Crystal Growth," Research Report #1, NASA Contract #NAS8-30250, August, 1974.

32. Zahn, M. and Melcher, J. R., "Space-Charge Dynamics of Liquids," Phys. Fluids, Vol. 15, July, 1972, pp. 1197-1206.

33. Reger, J. L., "Study on Processing Immiscible Materials in Zero Gravity," Interim Report, NASA Contract NAS8-28267, May, 1973.

APPENDIX A

(Abstract of paper which appeared in Journal of Applied Physics, Vol. 45, April, 1974, pp. 1487-1491)

HYDROSTATICS AND STEADY DYNAMICS OF SPATIALLY VARYING ELECTROMECHANICAL FLOW STRUCTURES

by Thomas B. Jones
Department of Electrical Engineering
Colorado State University
Ft. Collins, CO 80523

The hydrostatic and steady laminar hydrodynamic equilibria of spatially varying electromechanical flow structures are investigated. Under certain conditions the relationship between the dielectric height of rise and the applied voltage is found to be double valued. It is found that one of the two equilibrium values is always unstable. This gives rise to the experimentally observed spontaneous rise of the fluid to the top of the structure, once a certain critical voltage is reached. Starting above this critical voltage with the structure completely filled and decreasing the applied voltage toward the critical value results in pinch-in failure at an intermediate point along the structure and trapping of dielectric fluid at the top. The simple mathematical model developed predicts all these phenomena, without recourse to tedious point-by-point surface force equilibrium determination. Experiments are reported which verify the results for the hydrostatic case.

Appendix B

Description of Pressure Vessel designed, built and used in Experimental Electrohydrodynamic Liquid Handling Experiments

A pressure vessel was designed and built as part of this research project. The facility is unique in that it has high voltage electrical feedthroughs, as well as low voltage feedthroughs, and observation ports. The configuration is cylindrical, with two observation ports mounted at a 90° angle with respect to each other. The inside vessel diameter is 11 1/2", and the inside vertical length is 14". The top is a blind flange, which can be removed to give access to the inside. The pressure vessel is designed to a maximum 450 psig, with a substantial safety factor. Two 50 kV high voltage electrical feedthroughs, and four low voltage feedthroughs, are mounted on the top flange. The pressure vessel is shown in Figure B.1.

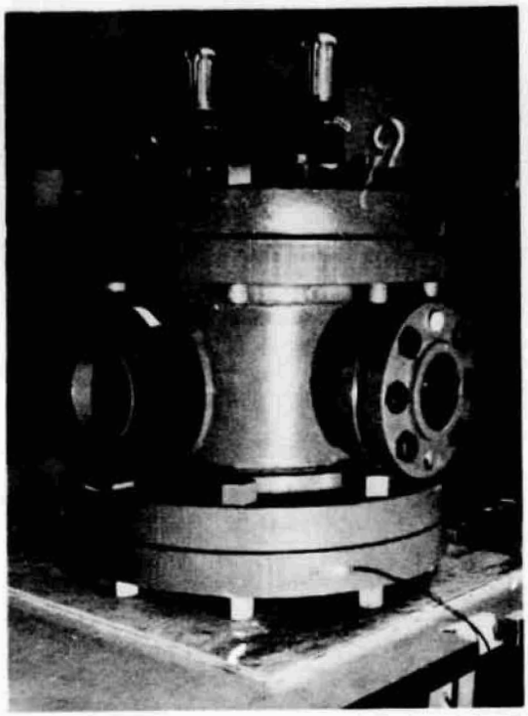

Figure B.1 Pressure Vessel with Observation Ports and High Voltage Feedthroughs Shown

NOMENCLATURE

$\bar{a}$	-	acceleration
c	-	specific heat
C	-	drag coefficient for sphere
$\bar{E}$	-	electric field strength
$\bar{E}_b$	-	breakdown electric fluid strength
f	-	electric field frequency
$\bar{f}^e$	-	electrical body force density
$\bar{F}$	-	force
g	-	gravitational acceleration ($9.81 \frac{m}{sec}2$)
g'	-	effective gravitational acceleration
h	-	dielectric height of rise
$\bar{J}$	-	current density
ℓ	-	long dimension of parallel-plate electrohydrodynamic liquid orientation structure
$\dot{m}$	-	mass flow rate
p_ℓ	-	liquid hydrostatic pressure
p_o	-	ambient hydrostatic pressure
P_{diss}	-	ohmic power dissipated per unit volume
r	-	radius of dielectric spheres or bubbles
t	-	time
T	-	temperature
$\frac{dT}{dt}$	-	time rate of change of temperature
V	-	voltage

w - electrode plate width

γ - surface tension

ϵ - dielectric permittivity

μ - dynamic viscosity

ξ - liquid surface displacement

ρ - liquid density

ρ_f - free charge volume densit

η - kinematic viscosity $(\frac{\mu}{\rho})$

σ - electrical conductivity

τ - charge relaxation time constant $(\frac{\epsilon}{\sigma})$

τ_m - electric-viscous time $(\frac{\mu}{\sigma E^2})$